Neural-Network-Based Adaptive Optimized Finite-time Control of Switched Systems with Constraints

Fatemeh Kamali, Mohammad Farrokhi*

Abstract—This paper presents a finite-time optimized backstepping control strategy for uncertain strict-feedback switched systems subject to full-state constraints. The proposed method integrates adaptive backstepping, Nonlinear Mapping (NM), and reinforcement learning (RL) to achieve enhanced control performance. The NM technique is employed to prevent constraint violations and to relax the feasibility conditions. The RL framework adopts an identifier–actor–critic architecture, where the identifier estimates the unknown dynamics, the actor generates control inputs, and the critic evaluates system performance. To enhance computational efficiency, a simplified RL algorithm is developed, in which the update laws for the actor–critic network weights are derived from the negative gradient of a positive-definite function obtained through the partial derivative of the Hamilton–Jacobi–Bellman (HJB) equation. Simulation results demonstrate that the proposed control method achieves superior performance compared to state-of-the-art methods reported in recent literature.

Index Terms—Adaptive optimized backstepping, finite-time control, identifier-actor-critic neural networks, switched systems, full-state constraints

I. INTRODUCTION

In modern engineering, many real-world systems—such as networked control systems [1], reactors [2], and aircraft [3]—exhibit switching behaviors due to operational mode changes, component switching, or reconfiguration. These systems, typically modeled as switched nonlinear systems, consist of multiple subsystems with distinct dynamic characteristics, governed by a switching signal that determines which subsystem is active at each instant. The switching can occur arbitrarily, either as a result of external commands or internal events, thereby introducing significant challenges for controller design [4]. Therefore, developing adaptive control strategies that ensure stability and desired performance under arbitrary switching has become a crucial research direction in nonlinear control.

Among various techniques, adaptive backstepping control has emerged as a systematic and effective approach for handling uncertain nonlinear systems. In this method, uncertain elements are commonly approximated using neural networks (NNs) or fuzzy logic [4]–[7]. However, traditional backstepping methods often achieve the control objective as time approaches infinity, which may not be satisfactory for applications that demand fast transient responses. To overcome this limitation, finite-time control strategies have been developed, enabling convergence of tracking errors within a finite time, and thereby enhancing system transient performance and robustness against disturbances and noise [8], [9].

In addition, practical systems often operate under state constraints imposed by physical limitations or safety requirements. To handle such constraints within the backstepping framework, two main approaches have been proposed: Barrier Lyapunov Functions (BLFs) [10]–[12] and Nonlinear Mappings (NMs) [13]. Among the BLF-based methods, the most widely used are the Logarithmic BLF (Log-BLF) [14]–[17] due to its simplicity, the Tangent BLF (Tan-BLF) [18]–[21], and the Integral BLF (IBLF) [22]. A major challenge in BLF-based methods is maintaining the feasibility condition, as the virtual control signal must also satisfy the constraints, which becomes particularly difficult in the presence of system uncertainties. On the other hand, NM-based methods are often more straightforward, as they do not require explicit feasibility conditions, thus making parameter tuning simpler and more flexible [23]–[25].

Constrained control and finite-time control each offer distinct advantages when applied independently. Integrating these two approaches to design a finite-time constrained controller introduces additional complexities. However, it enhances the controller's practicality. Consequently, the design of constrained finite-time controllers has become an important research topic and has attracted increasing attention in recent years, although relatively few studies have been conducted for switched systems in this area. For instance, in [26], a fault-tolerant finite-time controller was developed for constrained multi-input–multi-output (MIMO) systems with asymmetric and time-varying output constraints. A Log-BLF was employed to ensure system stability in the presence of these constraints.

Similarly, in [6], a multi-objective constrained finite-time control scheme with time-varying and asymmetric constraints was proposed, again employing a BLF to maintain stability. In [27], finite-time control was designed for output-feedback systems with quantized inputs and symmetric, time-invariant output constraints, where a Log-BLF was utilized in the controller design. Furthermore, in [7], a Tan-BLF-based finite-time control approach was applied to a strict-feedback system with symmetric and time-invariant state constraints. In [28], Log-BLF finite-time control was developed for switched systems with constant and symmetric constraints, while [29] extended this framework to switched systems with zero dynamics. In [30], a Tan-BLF was used for finite-time control under time-varying, yet symmetric constraints.

Although constrained finite-time backstepping control enables the design of practical controllers, it often results in high resource utilization and consequently increases implementation costs. This has motivated the consideration of optimal control, which aims

* The authors are with the School of Electrical Engineering, Iran University of Science and Technology, Tehran 16846, Iran (e-mail: farrokhi@iust.ac.ir)

to reduce control effort while maintaining the desired performance. Optimal control plays a crucial role in many engineering applications, offering benefits in terms of performance, efficiency, and resource allocation [31].

While optimal control has been widely explored in various control algorithms, optimal backstepping control has received comparatively less attention due to its analytical complexity. Recently, some efforts have been made to optimize the backstepping controllers. For example, in [32] an actor–critic reinforcement learning (RL) structure was integrated into backstepping control to optimize non-switching systems. In this method, the actor network is trained to ensure system stability, while the critic network is tuned by minimizing the Hamilton–Jacobi–Bellman (HJB) equation. In [33], an algorithm was developed to simplify the optimization process of backstepping control. Instead of using the squared error of the HJB approximation, the method utilizes the negative gradient of a simple positive-definite function derived from the partial derivative of the HJB equation. This approach significantly reduces computational complexity and is therefore referred to as the simplified optimal backstepping method**.** The simplified optimal backstepping approach has been investigated in a few studies. For instance, in [34], it was used to control uncertain constrained systems with symmetric, time-invariant state constraints, where tangent BLFs replaced standard quadratic Lyapunov functions, and Radial-Basis-Function Neural Networks (RBFNNs) were employed to estimate system uncertainties.

In [35], the method was applied to unmanned aerial vehicles, and in [36], to strict-feedback multi-agent systems. Reference [37] extended the approach to ensure system performance during transient phases in unmanned submarines. In [38], an optimal backstepping controller was designed for a strict-feedback system with output feedback and dynamic uncertainty, where a NN was used to estimate the uncertainties and an observer was used to estimate the states. In [39], optimal backstepping was developed for systems with uncertain control gains. In [40], a simplified optimal backstepping algorithm was applied to an output-feedback system, where fuzzy logic was employed both to estimate uncertainties and as a state observer. In [41], the simplified optimal backstepping algorithm was extended to strict-feedback systems with output constraints and external disturbances, employing a NN to estimate uncertainties and disturbances, and a BLF to prevent constraint violations.

The aforementioned studies focus on non-switched systems. Optimal backstepping control for switched systems has been investigated in only a limited number of works. In [42] optimal backstepping was applied to switched systems along with a fuzzy estimator to handle system uncertainties under arbitrary switching. In [43], an optimal backstepping control was developed for a constrained switching system, where an actor–critic network was integrated with a Log-BLF to achieve both optimal performance and constraint satisfaction.

Motivated by the above considerations, this paper proposes a novel adaptive finite-time control scheme for switched strict-feedback nonlinear systems with full-state constraints under arbitrary switching. The proposed design integrates the advantages of backstepping, NM, and an actor–critic NN framework to achieve fast convergence, optimized control performance, and guaranteed constraint satisfaction. The developed controller ensures that all closed-loop signals remain bounded and that the tracking error converges to a small neighborhood of the origin in a finite time, even under arbitrary switching among subsystems with uncertain dynamics. The main contributions of this work are summarized as follows:

1. For the first time, a novel optimized adaptive finite-time backstepping control framework is developed for switched strict-feedback nonlinear systems, capable of handling arbitrary switching while ensuring finite-time convergence.
2. NM is employed to effectively handle full-state constraints, guaranteeing that the system states remain within their admissible bounds during operation. The feasibility conditions considered in previous works, such as [6], [7], [27] and [43] are relaxed. Furthermore, the constraints do not need to have specific forms, such as being symmetric or constant; they can take any general form as long as their time-derivatives exist.
3. An RL actor–critic NN structure is incorporated to optimize the adaptive control policy. The RL algorithm is designed based on the negative gradient of a simple positive-definite function, which is generated from the partial derivative of the HJB equation. It can significantly simplify optimal control and also relaxes the persistence of excitation required in previous works; e.g., [32] and [43].

The rest of the paper is organized as follows. Section 2 presents the dynamics of the system and introduces the basic concepts. Section 3 details the design of the optimal finite-time controller design for constrained systems. Section 4 demonstrates the performance of the proposed controller, and finally, Section 5 provides the conclusion.

II. SYSTEM DESCRIPTION AND BASIC KNOWLEDGE

Consider the following switched strict-feedback systems [22]:

$$\begin{aligned} \dot{x}_i &= f_i^{\sigma}(\bar{\mathbf{x}}_i) + g_i^{\sigma}(\bar{\mathbf{x}}_i)x_{i+1} \quad i = 1,...,n-1 \\ \dot{x}_n &= f_n^{\sigma}(\bar{\mathbf{x}}_n) + u \\ y &= x_1 \end{aligned} \tag{1}$$

where $\bar{\mathbf{x}}_i = [x_1,\dots,x_i]^T \in R^i$, $\bar{\mathbf{x}}_n = [x_1,\dots,x_n]^T \in R^n$ represent the state vector, n is the number of the system states, $u \in R$ and $y \in R$ denote the system's input and output, respectively, f_i^{σ} and f_n^{σ} are continuous and locally Lipschitz functions, g_i^{σ} is continuous function and non-zero at all times with constant and known signs; $\sigma : R^+ \rightarrow \varsigma = \{1, 2, \dots, \varsigma\}$ denotes the switching signal and ς represents the number of switching subsystems.

The control objective is to design a controller for system (1) based on the optimized backstepping technique such that:

1. All signals in the closed-loop system remain bounded.
2. Each state remains within the defined constraints, as

$$\underline{c}_i < x_i < \bar{c}_i \ , \ i = 1,\dots,n \tag{2}$$

where $\underline{c}_i$ and $\bar{c}_i$ are continues and known functions of time.

Remark 1: It should be emphasized that the states, input, output, switching signal and constraints are time-dependent. This time dependency is omitted for simplicity.

To achieve the control goals, a set of assumptions and lemmas are introduced in the followings.

Assumption 1: it is assumed that the function g_i^σ is nonsingular and its sign is known. Without loss of generality, it is assumed that g_i^σ is positive, which implies that for every σ, there exist positive constants g_i^0 such that

$$0 < g_i^0 < g_i^\sigma(\bar{\mathbf{x}}_i),\ i = 1,\dots,n,\ \sigma \in \varsigma \tag{3}$$

Remark 2: Assumption 1 is widely adopted in many existing studies, such as [4], [24], [23].

Assumption 2: The reference y_d and its derivative up to nth order are bounded. Furthermore, the desired output does not violate the constraints which implies that there exist $\underline{c}_d(t)$ and $\bar{c}_d(t)$ such that

$$\underline{c}_1 < \underline{c}_d(t) < y_d < \bar{c}_d(t) < \bar{c}_1 \tag{4}$$

Lemma 1 [44]: The RBFNN can approximate any continuous unknown function $\mathbf{h}(\mathbf{X}): R^n \to R^m$ in closed space Ω_X. It means that there exists a NN such that for $\forall e > 0$

$$\mathbf{h}(\mathbf{X}) = \mathbf{W}^{*T}\boldsymbol{\phi}(\mathbf{X}) + \boldsymbol{\varepsilon},\quad |\boldsymbol{\varepsilon}| < e \tag{5}$$

where $\mathbf{X} \in \Omega_X \subset R^n$ is input vector, $\boldsymbol{\varepsilon} \in R^m$ represents the approximation error and e is its upper bound, $\boldsymbol{\phi}(\mathbf{X})$ is the vector of radial-basis functions, and $\mathbf{W}^*$ is the vector of ideal weights satisfying

$$\mathbf{W}^* = \arg\min_{\mathbf{W}} \left|\mathbf{h}(\mathbf{X}) - \mathbf{W}^T\boldsymbol{\phi}(\mathbf{X})\right|. \tag{6}$$

in which $\mathbf{W} \in R^{l\times m}$ denotes the vector of actual weights and the elements of $\boldsymbol{\phi}(\mathbf{X}) = [\varphi_1(\mathbf{X}),\dots,\varphi_l(\mathbf{X})]^T$ can be expressed as

$$\varphi_i(\mathbf{X}) = \exp\left[-\frac{(\mathbf{X}-\boldsymbol{\mu}_i)^T(\mathbf{X}-\boldsymbol{\mu}_i)}{\eta_i^2}\right] \quad i = 1,\dots,l \tag{7}$$

where $\boldsymbol{\mu}_i = [\boldsymbol{\mu}_{i1},\dots,\boldsymbol{\mu}_{in}]^T$ and η_i are the center and width of the Gaussian functions, respectively, and l is the number of neurons in the hidden layer.

Lemma 2 (Young's inequality) [45]: for any real numbers a and b, the following inequality holds:

$$ab \le \frac{\eta^{\varpi_1}}{\varpi_1}|a|^{\varpi_1} + \frac{1}{\eta^{\varpi_2}\varpi_2}|b|^{\varpi_2} \tag{8}$$

where $\eta > 0$, $\varpi_1 > 1$, $\varpi_2 > 1$, and $(\varpi_1 - 1)(\varpi_2 - 1) = 1$.

Lemma 3 [46]: For real variables ν_1 and ν_2, and positive constants ι_1, ι_2, and ι_3, the following inequality holds:

$$|\nu_1|^{\iota_1}|\nu_2|^{\iota_2} \le \frac{\iota_1}{\iota_1+\iota_2}\iota_3|\nu_1|^{\iota_1+\iota_2} + \frac{\iota_2}{\iota_1+\iota_2}\iota_3^{-\iota_1/\iota_2}|\nu_2|^{\iota_1+\iota_2} \tag{9}$$

Lemma 4 [47]: Consider the system $\dot{\boldsymbol{\chi}} = f(\boldsymbol{\chi})$. If there exists a continuous function $V(\boldsymbol{\chi})$ such that

$$\dot{V}(\boldsymbol{\chi}) < -\rho_1 V^p(\boldsymbol{\chi}) - \rho_2 V(\boldsymbol{\chi}) + \rho_3 \tag{10}$$

where $\rho_1 > 0$, $\rho_2 > 0$, $0 < \rho_3 < \infty$, and $0 < p < 1$, then the system is finite-time stable. In addition, the upper bound of the settling-time is given by

$$T_r < \max\left\{\begin{array}{l} t_0 + \dfrac{1}{\lambda\rho_2(1-p)}\ln\dfrac{\lambda\rho_2 V^{1-p}(t_0)+\rho_1}{\rho_1}, \\ t_0 + \dfrac{1}{\rho_2(1-p)}\ln\dfrac{\rho_2 V^{1-p}(t_0)+\lambda\rho_1}{\lambda\rho_1} \end{array}\right\}. \tag{11}$$

Moreover,

$$\lim_{t\to T_r} V(\boldsymbol{\chi}) \le \min\left\{\frac{\rho_3}{(1-\lambda)\rho_2}, \left(\frac{\rho_3}{(1-\lambda)\rho_2}\right)^{1/p}\right\} \tag{12}$$

where $0 < \lambda < 1$ and t_0 is the initial time.

III. CONTROLLER DESIGN

To develop an optimized finite-time controller for the strict-feedback switched system given in (1) under constraints given in (2), the following NM is proposed:

$$\xi_i := \ln \frac{\underline{c}_i + x_i}{\overline{c}_i - x_i} \tag{13}$$

whose inverse is given as

$$x_i = \overline{c}_i - \frac{\overline{c}_i + \underline{c}_i}{e^{\xi_i} + 1}. \tag{14}$$

Therefore,

$$\dot{\xi}_i = \frac{e^{\xi_i} + e^{-\xi_i} + 2}{\overline{c}_i + \underline{c}_i} \dot{x}_i + \frac{\dot{\underline{c}}_i (e^{-\xi_i} + 1) - \dot{\overline{c}}_i (e^{\xi_i} + 1)}{\overline{c}_i + \underline{c}_i}. \tag{15}$$

Using (15), the switched system in (1) is transformed into

$$\begin{aligned} \dot{\xi}_i &= \mathfrak{F}_i^{\sigma}\left(\overline{\boldsymbol{\xi}}_{i+1}\right) + \xi_{i+1}, \quad i = 1, \ldots, n-1 \\ \dot{\xi}_n &= \mathfrak{F}_n^{\sigma}\left(\overline{\boldsymbol{\xi}}_n\right) + \mathfrak{G}_n(\overline{\boldsymbol{\xi}}_n) u \\ \mathfrak{Y} &= \xi_1 \end{aligned} \tag{16}$$

where

$\mathfrak{F}_i^{\sigma} = k_{1i}\left[f_i^{\sigma}(\overline{\mathbf{x}}_i) + g_i^{\sigma}(\overline{\mathbf{x}}_i) x_{i+1}\right] + k_{2i} - \xi_{i+1}$ $\quad \mathfrak{F}_n^{\sigma} = k_{1n} f_n^{\sigma}(\overline{\mathbf{x}}_n) + k_{2n}$, $\quad \mathfrak{G}_n = k_{1n}$, $\quad k_{1i} := \dfrac{e^{\xi_i} + e^{-\xi_i} + 2}{\overline{c}_i + \underline{c}_i}$

$k_{2i} := \dfrac{\dot{\underline{c}}_i (e^{-\xi_i} + 1) - \dot{\overline{c}}_i (e^{\xi_i} + 1)}{(\overline{c}_i + \underline{c}_i)}$, $k_{1n} := \dfrac{e^{\xi_n} + e^{-\xi_n} + 2}{\overline{c}_n + \underline{c}_n}$ $k_{2n} := \dfrac{\dot{\underline{c}}_n (e^{-\xi_n} + 1) - \dot{\overline{c}}_n (e^{\xi_n} + 1)}{(\overline{c}_n + \underline{c}_n)}$.

Moreover, the mapped desired output is defined as follows:

$$\Upsilon_d := \log \frac{\underline{c}_1 + y_d}{\overline{c}_1 - y_d} \tag{17}$$

Remark 3: By applying the NM defined in (13), the constrained system in (1) is converted into the unconstrained system described in (16). This transformation simplifies the controller design process as it allows the control law to be developed for an unconstrained system. In addition, the resulting controller can be effectively applied to the control system in (1) while ensuring that all state constraints are satisfied.

To design a controller for system (16) based on the backstepping method, the following steps are taken.

Step 1: The tracking error is defined as $z_1 := \xi_1 - \Upsilon_d$ and $z_2 := \xi_2 - \alpha_1$. According to the transformed system, the following dynamic equation is derived:

$$\dot{z}_1 = \dot{\xi}_1 - \dot{\Upsilon}_d = z_2 + \alpha_1 + \mathfrak{F}_1^{\sigma}\left(\overline{\boldsymbol{\xi}}_2\right) - \dot{\Upsilon}_d. \tag{18}$$

The optimal value function is defined as

$$J_1^* := \min_{\alpha_1}\left(\int_t^{\infty} h_1\left(z_1(s), \alpha_1(s) ds\right)\right) = \int_t^{\infty} h_1\left(z_1(s), \alpha_1^*(s) ds\right) \tag{19}$$

where $h_1(z_1, \alpha_1) = z_1^2 + \alpha_1^2$ is the local cost function, α_1 is the virtual controller and α_1^* is its optimal value. Using (19), the HJB equation can be obtained as follows:

$$H_1 = z_1^2 + \alpha_1^{*2} + \frac{dJ_1^*(z_1)}{dz_1}\left(z_2 + \alpha_1^* + \mathfrak{F}_1^{\sigma}\left(\overline{\boldsymbol{\xi}}_2\right) - \dot{\Upsilon}_d\right) = 0. \tag{20}$$

From (20), the optimal virtual controller can be obtained as

$$\alpha_1^* = -\frac{1}{2}\frac{dJ_1^*(z_1)}{dz_1}. \tag{21}$$

Using (21), (20) can be rewritten as follows:

$$H_1(z_1, \alpha_1^*, \frac{dJ_1^*}{dz_1}) = z_1^2 + \left(\frac{1}{2}\frac{dJ_1^*(z_1)}{dz_1}\right)^2 + \frac{dJ_1^*(z_1)}{dz_1}\left(z_2 - \frac{1}{2}\frac{dJ_1^*(z_1)}{dz_1} + \mathfrak{F}_1^{\sigma}\left(\overline{\boldsymbol{\xi}}_2\right) - \dot{\Upsilon}_d\right) = 0 \tag{22}$$

Solving this nonlinear differential equation is not trivial. To overcome this problem, NNs are employed. First, a NN is utilized to approximate the unknown function $F_1^{\sigma}(\bar{\xi}_2) =: \mathfrak{F}_1^{\sigma}(\bar{\xi}_2)$, as shown below; this network will hereafter be referred to as the *identifier network*:

$$\begin{aligned}&\boldsymbol{\phi}_{f1} = \boldsymbol{\phi}_f\left(\mathbf{X}_{f1}\right)\\ &F_1^{\sigma}\left(\mathbf{X}_{f1}\right) = \mathbf{W}_{f1}^{*\sigma T}\boldsymbol{\phi}_{f1} + \varepsilon_{f1}^{\sigma}, \quad \left|\varepsilon_{f1}^{\sigma}\right| < e_{f1}\end{aligned} \tag{23}$$

where $\mathbf{W}_{f1}^{*\sigma}$ is the ideal weights of the identifier NN, $\boldsymbol{\phi}_f$ is the basis-function vector, $\varepsilon_{f1}^{\sigma}$ is the approximation error and e_{f1} is its upper bound, $\mathbf{X}_{f1} = (\bar{\xi}_2)$ is the input to this network.

Next, define $\theta_{f1}^{*} := \max\{\| \mathbf{W}_{f1}^{*\sigma} \|\}$ where θ_{f1} is its estimation. Define $J_1^{o}(\bar{\xi}_2, z_1)$ as

$$J_1^{o}(\bar{\xi}_2, z_1) := \frac{dJ_1^{*}}{dz_1} - 2r_{11}z_1^{2p-1} - 2r_{12}z_1 - \frac{1}{\eta_1^2}z_1\theta_{f1}^{*}\boldsymbol{\phi}_{f1}^{T}\boldsymbol{\phi}_{f1} \tag{24}$$

where dJ_1^{*}/dz_1 can be obtained as

$$\frac{dJ_1^{*}}{dz_1} = 2r_{11}z_1^{2p-1} + 2r_{12}z_1 + \frac{1}{\eta_1^2}z_1\theta_{f1}^{*}\boldsymbol{\phi}_{f1}^{T}\boldsymbol{\phi}_{f1} + J_1^{o}(\bar{\xi}_2, z_1)\,. \tag{25}$$

By substituting (25) into (21), it gives

$$\alpha_1^{*} = -\frac{1}{2}J_1^{o}(\bar{\xi}_2, z_1) - r_{11}z_1^{2p-1} - r_{12}z_1 - \frac{1}{2\eta_1^2}z_1\theta_{f1}^{*}\boldsymbol{\phi}_{f1}^{T}\boldsymbol{\phi}_{f1} \tag{26}$$

where r_{11}, r_{12} and η_1 are positive design constants and $0 < p < 1$. In (26), $J_1^{o}(\bar{\xi}_2, z_1)$ and θ_{f1}^{*} are unknown. Hence, this controller cannot be applied to the system. To resolve this problem, a NN is used to estimate J_1^{o} as follows:

$$\begin{aligned}&\boldsymbol{\phi}_{J1} = \boldsymbol{\phi}_J\left(\mathbf{X}_{J1}\right)\\ &J_1^{o}(\bar{\xi}_2, z_1) = \mathbf{W}_{J1}^{*T}\boldsymbol{\phi}_{J1} + \varepsilon_{J1}, \quad \left|\varepsilon_{J1}\right| < e_{J1}\end{aligned} \tag{27}$$

where $\mathbf{W}_{J1}^{*T}$ are the ideal weights, $\boldsymbol{\phi}_J$ is the basis-function vector, $\varepsilon_{J1}^{\sigma}$ is the approximation error and e_{J1} is its upper bound, and $\mathbf{X}_{J1} = (\mathbf{X}_{f1}, z_1)$. Substituting (27) into (25) and (26), results in

$$\frac{dJ_1^{*}}{dz_1} = 2r_{11}z_1^{2p-1} + 2r_{12}z_1 + \frac{1}{\eta_1^2}z_1\theta_{f1}^{*}\boldsymbol{\phi}_{f1}^{T}\boldsymbol{\phi}_{f1} + W_{J1}^{*T}\boldsymbol{\phi}_{J1} \tag{28}$$

$$\alpha_1^{*} = -\frac{1}{2}\mathbf{W}_{J1}^{*T}\boldsymbol{\phi}_{J1} - r_{11}z_1^{2p-1} - r_{12}z_1 - \frac{1}{2\eta_1^2}z_1\theta_{f1}^{*}\boldsymbol{\phi}_{f1}^{T}\boldsymbol{\phi}_{f1} \tag{29}$$

Since the optimal weights ($\mathbf{W}_{J1}^{*}$ and θ_{f1}^{*}) are unknown, the controller in (29) cannot be directly implemented. To tackle this issue, an actor–critic NN is introduced as follows:

$$\frac{d\hat{J}_1^{*}}{dz_1} = 2r_{11}z_1^{2p-1} + 2r_{12}z_1 + \mathbf{W}_{c1}^{T}\boldsymbol{\phi}_{J1} + \frac{1}{\eta_1^2}z_1\theta_{f1}\boldsymbol{\phi}_{f1}^{T}\boldsymbol{\phi}_{f1} \tag{30}$$

$$\hat{\alpha}_1^{*} = -\frac{1}{2}\mathbf{W}_{a1}^{T}\boldsymbol{\phi}_{J1} - r_{11}z_1^{2p-1} - r_{12}z_1 - \frac{1}{2\eta_1^2}z_1\theta_{f1}\boldsymbol{\phi}_{f1}^{T}\boldsymbol{\phi}_{f1} \tag{31}$$

where $\mathbf{W}_{a1}$ is the actor and $\mathbf{W}_{c1}$ is the critic NN weights. As a result, the HJB approximation can be obtained as

$$\begin{aligned}H_1(z_1, \hat{\alpha}_1^{*}, \frac{d\hat{J}_1^{*}}{dz_1}) = z_1^2 &+ \left(\frac{1}{2}\mathbf{W}_{a1}^{T}\boldsymbol{\phi}_{J1} + r_{11}z_1^{2p-1} + r_{12}z_1 + \frac{1}{2\eta_1^2}z_1\theta_{f1}\boldsymbol{\phi}_{f1}^{T}\boldsymbol{\phi}_{f1}\right)^2\\ &+ \left(2r_{11}z_1^{2p-1} + 2r_{12}z_1 + \frac{1}{\eta_1^2}z_1\theta_{f1}\boldsymbol{\phi}_{f1}^{T}\boldsymbol{\phi}_{f1} + \mathbf{W}_{c1}^{T}\boldsymbol{\phi}_{J1}\right)\\ &\left(z_2 - \frac{1}{2}\mathbf{W}_{a1}^{T}\boldsymbol{\phi}_{J1} - r_{11}z_1^{2p-1} - r_{12}z_1 - \frac{1}{2\eta_1^2}z_1\theta_{f1}\boldsymbol{\phi}_{f1}^{T}\boldsymbol{\phi}_{f1} + \mathbf{W}_{f1}^{*\sigma T}\boldsymbol{\phi}_{f1} + \varepsilon_{f1}^{\sigma} - \dot{\Upsilon}_d\right)\end{aligned} \tag{32}$$

According to the HJB equation in (22) and its approximation in (32), the Bellman residual error $e_1(t)$ can be written as follows:

$$e_1 = H_1(z_1, \hat{\alpha}_1^{*}, \frac{d\hat{J}_1^{*}}{dz_1}) - H_1(z_1, \alpha_1^{*}, \frac{dJ_1^{*}}{dz_1})\,. \tag{33}$$

According to [33], the optimal controller is expected to minimize e_1. Given that $H_1(z_1, \alpha_1^{*}, dJ_1^{*}/dz_1) = 0$, it is expected that the optimal controller satisfies $H_1(z_1, \hat{\alpha}_1^{*}, d\hat{J}_1^{*}/dz_1) \to 0$. Since the HJB equation has a unique solution, the controller that minimize e_1 must satisfy the following equation:

$$\frac{\partial H_1(z_1, \hat{\alpha}_1^*, \frac{d\hat{J}_1^*}{dz_1})}{\partial \mathbf{W}_{a1}} = \frac{1}{2}\boldsymbol{\phi}_{J1}\boldsymbol{\phi}_{J1}^T\left(\mathbf{W}_{a1} - \mathbf{W}_{c1}\right) = 0 \,. \tag{34}$$

In order to derive the update laws for the actor-critic network that guarantees (34), a positive-definite function is defined as

$$P_1(t) := \left(\mathbf{W}_{a1} - \mathbf{W}_{c1}\right)^T \left(\mathbf{W}_{a1} - \mathbf{W}_{c1}\right). \tag{35}$$

It is obvious that $P_1(t) = 0$ is equal to (34). Considering that $\partial P_1/\partial \mathbf{W}_{a1} = -\partial P_1/\partial \mathbf{W}_{c1} = 2\left(\mathbf{W}_{a1} - \mathbf{W}_{c1}\right)$, the derivative of $P_1(t)$ becomes

$$\frac{dP_1}{dt} = \frac{\partial P_1}{\partial \mathbf{W}_{c1}^T}\dot{\mathbf{W}}_{c1} + \frac{\partial P_1}{\partial \mathbf{W}_{a1}^T}\dot{\mathbf{W}}_{a1} \,. \tag{36}$$

The update laws for the weights of the actor and critic networks are defined as follows:

$$\dot{\mathbf{W}}_{a1} := -\frac{1}{2}\delta_{z1}\boldsymbol{\phi}_{J1}z_1 - \left(\boldsymbol{\phi}_{J1}\boldsymbol{\phi}_{J1}^T + \delta_{J1}\mathbf{I}\right)\left(\gamma_{a1}\left(\mathbf{W}_{a1} - \mathbf{W}_{c1}\right) + \gamma_{c1}\mathbf{W}_{c1}\right) \tag{37}$$

$$\dot{\mathbf{W}}_{c1} := -\frac{1}{2}\delta_{z1}\boldsymbol{\phi}_{J1}z_1 - \gamma_{c1}\left(\boldsymbol{\phi}_{J1}\boldsymbol{\phi}_{J1}^T + \delta_{J1}\mathbf{I}\right)\mathbf{W}_{c1} \tag{38}$$

where γ_{a1} and γ_{c1} are positive constants and δ_{J1} and δ_{z1} are small positive constants. As a result, the derivative of $P_1(t)$ becomes

$$\frac{dP_1}{dt} = -\frac{\gamma_{a1}}{2}\frac{\partial P_1}{\partial \mathbf{W}_{a1}^T}\left(\boldsymbol{\phi}_{J1}^T\boldsymbol{\phi}_{J1} + \delta_{J1}\mathbf{I}\right)\frac{\partial P_1}{\partial \mathbf{W}_{a1}} \le 0 \,. \tag{39}$$

Inequality (39) means that $P_1(t) = 0$ is eventually achieved and hence $H_1(z_1, \hat{\alpha}_1^*, d\hat{J}_1^*/dz_1) \to 0$.

For the stability analysis, a Lyapunov function is defined as

$$V_1 := \frac{1}{2}z_1^2 + \frac{1}{2}\tilde{\theta}_{f1}^2 + \frac{1}{2}\tilde{\mathbf{W}}_{a1}{}^T\tilde{\mathbf{W}}_{a1} + \frac{1}{2}\tilde{\mathbf{W}}_{c1}{}^T\tilde{\mathbf{W}}_{c1} \tag{40}$$

where $\tilde{\theta}_{f1} = \theta_{f1} - \theta_{f1}^*$, $\tilde{\mathbf{W}}_{a1} = \mathbf{W}_{a1} - \mathbf{W}_{J1}^*$, and $\tilde{\mathbf{W}}_{c1} = \mathbf{W}_{c1} - \mathbf{W}_{J1}^*$. Using the identifier NN in (23), virtual controller in (31), and the actor-critic update laws in (37) and (38), the derivative of (40) can be obtained as follows:

$$\begin{aligned}\dot{V}_1 = {} & z_1\left(z_2 - \frac{1}{2}\mathbf{W}_{a1}^T\boldsymbol{\phi}_{J1} - r_{11}z_1^{2p-1} - r_{12}z_1 - \frac{1}{2\eta_1^2}z_1\theta_{f1}\boldsymbol{\phi}_{f1}^T\boldsymbol{\phi}_{f1} + \mathbf{W}_{f1}^{*\sigma T}\boldsymbol{\phi}_{f1} + \varepsilon_{f1}^{\sigma} - \dot{\Upsilon}_d\right) \\ & + \tilde{\theta}_{f1}\dot{\theta}_{f1} - \tilde{\mathbf{W}}_{a1}^T\left(\frac{1}{2}\delta_{z1}\boldsymbol{\phi}_{J1}z_1 + \left(\boldsymbol{\phi}_{J1}\boldsymbol{\phi}_{J1}^T + \delta_{J1}\mathbf{I}\right)\left(\gamma_{a1}\left(\mathbf{W}_{a1} - \mathbf{W}_{c1}\right) + \gamma_{c1}\mathbf{W}_{c1}\right)\right) \\ & - \tilde{\mathbf{W}}_{c1}^T\left(\frac{1}{2}\delta_{z1}\boldsymbol{\phi}_{J1}z_1 + \gamma_{c1}\left(\boldsymbol{\phi}_{J1}\boldsymbol{\phi}_{J1}^T + \delta_{J1}\mathbf{I}\right)\mathbf{W}_{c1}\right).\end{aligned} \tag{41}$$

Using Lemma 2, the following inequalities are obtained:

$$z_1\varepsilon_{f1}^{\sigma} \le \frac{1}{2}z_1^2 + \frac{1}{2}e_{f1}^2 \tag{42}$$

$$-\frac{1}{2}z_1\mathbf{W}_{a1}^T\boldsymbol{\phi}_{J1} \le \frac{1}{4}z_1^2 + \frac{1}{4}\mathbf{W}_{a1}^T\left(\boldsymbol{\phi}_{J1}\boldsymbol{\phi}_{J1}^T + \delta_{J1}\mathbf{I}\right)\mathbf{W}_{a1} \tag{43}$$

$$-\frac{1}{2}z_1\delta_{z1}\tilde{\mathbf{W}}_{a1}^T\boldsymbol{\phi}_{J1} \le \frac{1}{4}z_1^2 + \frac{1}{4}\delta_{z1}^2\tilde{\mathbf{W}}_{a1}^T\left(\boldsymbol{\phi}_{J1}\boldsymbol{\phi}_{J1}^T + \delta_{J1}\mathbf{I}\right)\tilde{\mathbf{W}}_{a1} \tag{44}$$

$$-\frac{1}{2}z_1\delta_{z1}\tilde{\mathbf{W}}_{c1}^T\boldsymbol{\phi}_{J1} \le \frac{1}{4}z_1^2 + \frac{1}{4}\delta_{z1}^2\tilde{\mathbf{W}}_{c1}^T\left(\boldsymbol{\phi}_{J1}\boldsymbol{\phi}_{J1}^T + \delta_{J1}\mathbf{I}\right)\tilde{\mathbf{W}}_{c1} \tag{45}$$

$$z_1\mathbf{W}_{f1}^{*\sigma T}\boldsymbol{\phi}_{f1} \le \frac{1}{2}\eta_1^2 + \frac{1}{2\eta_1^2}z_1^2\theta_{f1}^*\boldsymbol{\phi}_{f1}^T\boldsymbol{\phi}_{f1} \tag{46}$$

$$-z_1\dot{\Upsilon}_d \le \frac{1}{2}z_1^2 + \frac{1}{2}\dot{\Upsilon}_d^2 \,. \tag{47}$$

By defining the adaptation law as

$$\dot{\theta}_{f1} := \frac{1}{2\eta_1^2}z_1^2\boldsymbol{\phi}_{f1}^T\boldsymbol{\phi}_{f1} - \delta_{f1}\theta_{f1} \tag{48}$$

and by substituting (42)–(48) into (41), it gives

$$\begin{aligned}\dot V_1 \le & -r_{11}z_1^{2p}-(r_{12}-\frac{7}{4})z_1^2-\delta_{f1}\tilde\theta_{f1}\theta_{f1}-\gamma_{c1}\tilde{\mathbf W}_{c1}^T\left(\phi_{J1}\phi_{J1}^T+\delta_{J1}\mathbf I\right)\mathbf W_{c1}\\ & -\gamma_{a1}\tilde{\mathbf W}_{a1}^T\left(\phi_{J1}\phi_{J1}^T+\delta_{J1}\mathbf I\right)\mathbf W_{a1}+(\gamma_{a1}-\gamma_{c1})\tilde{\mathbf W}_{a1}^T\left(\phi_{J1}\phi_{J1}^T+\delta_{J1}\mathbf I\right)\mathbf W_{c1}\\ & +\frac14\mathbf W_{a1}^T\left(\phi_{J1}\phi_{J1}^T+\delta_{J1}\mathbf I\right)\mathbf W_{a1}+\frac14\delta_z^2\tilde{\mathbf W}_{a1}^T\left(\phi_{J1}\phi_{J1}^T+\delta_{J1}\mathbf I\right)\tilde{\mathbf W}_{a1}\\ & +\frac14\delta_{z1}^2\tilde{\mathbf W}_{c1}^T\left(\phi_{J1}\phi_{J1}^T+\delta_{J1}\mathbf I\right)\tilde{\mathbf W}_{c1}+\frac12 e_{f1}^2+\frac12\dot\Upsilon_d^2+\frac12\eta_1^2+z_1z_2.\end{aligned} \tag{49}$$

where δ_{f1} is a positive constant. Based on the definition of $\tilde\theta_{f1}$, $\tilde{\mathbf W}_{c1}$, and $\tilde{\mathbf W}_{a1}$, the following equations are derived:

$$\tilde\theta_{f1}\theta_{f1}=\frac12\tilde\theta_{f1}^2+\frac12\theta_{f1}^2-\frac12\theta_{f1}^{*2} \tag{50}$$

$$\tilde{\mathbf W}_{c1}^T\left(\phi_{J1}\phi_{J1}^T+\delta_{J1}\mathbf I\right)\mathbf W_{c1}=\frac12\tilde{\mathbf W}_{c1}^T\left(\phi_{J1}\phi_{J1}^T+\delta_{J1}\mathbf I\right)\tilde{\mathbf W}_{c1}+\frac12\mathbf W_{c1}^T\left(\phi_{J1}\phi_{J1}^T+\delta_{J1}\mathbf I\right)\mathbf W_{c1}-\frac12\mathbf W_{J1}^{*T}\left(\phi_{J1}\phi_{J1}^T+\delta_{J1}\mathbf I\right)\mathbf W_{J1}^* \tag{51}$$

$$\tilde{\mathbf W}_{a1}^T\left(\phi_{J1}\phi_{J1}^T+\delta_{J1}\mathbf I\right)\mathbf W_{a1}=\frac12\tilde{\mathbf W}_{a1}^T\left(\phi_{J1}\phi_{J1}^T+\delta_{J1}\mathbf I\right)\tilde{\mathbf W}_{a1}+\frac12\mathbf W_{a1}^T\left(\phi_{J1}\phi_{J1}^T+\delta_{J1}\mathbf I\right)\mathbf W_{a1}-\frac12\mathbf W_{J1}^{*T}\left(\phi_{J1}\phi_{J1}^T+\delta_{J1}\mathbf I\right)\mathbf W_{J1}^* \tag{52}$$

Applying Lemma 2 yields

$$(\gamma_{a1}-\gamma_{c1})\tilde{\mathbf W}_{a1}^T\left(\phi_{J1}\phi_{J1}^T+\delta_{J1}\mathbf I\right)\mathbf W_{c1}\le\frac{(\gamma_{a1}-\gamma_{c1})}{2}\tilde{\mathbf W}_{a1}^T\left(\phi_{J1}\phi_{J1}^T+\delta_{J1}\mathbf I\right)\tilde{\mathbf W}_{a1}+\frac{(\gamma_{a1}-\gamma_{c1})}{2}\mathbf W_{c1}\left(\phi_{J1}\phi_{J1}^T+\delta_{J1}\mathbf I\right)\mathbf W_{c1} \tag{53}$$

By substituting (50)–(53) into (49), it yields

$$\begin{aligned}\dot V_1 \le & -r_{11}z_1^{2p}-(r_{12}-\frac74)z_1^2-\frac{\delta_{f1}}{2}\tilde\theta_{f1}^2-\left(\frac{\gamma_{c1}}{2}-\frac14\delta_{z1}^2\right)\tilde{\mathbf W}_{c1}\left(\phi_{J1}\phi_{J1}^T+\delta_{J1}\mathbf I\right)\tilde{\mathbf W}_{c1}\\ & -\left(\frac{\gamma_{c1}}{2}-\frac14\delta_{z1}^2\right)\tilde{\mathbf W}_{a1}^T\left(\phi_{J1}\phi_{J1}^T+\delta_{J1}\mathbf I\right)\tilde{\mathbf W}_{a1}-\left(\gamma_{c1}-\frac{\gamma_{a1}}{2}\right)\mathbf W_{c1}^T\left(\phi_{J1}\phi_{J1}^T+\delta_{J1}\mathbf I\right)\mathbf W_{c1}\\ & -\left(\frac{\gamma_{a1}}{2}-\frac14\right)\mathbf W_{a1}^T\left(\phi_{J1}\phi_{J1}^T+\delta_{J1}\mathbf I\right)\mathbf W_{a1}+\left(\frac{\gamma_{c1}}{2}+\frac{\gamma_{a1}}{2}\right)\mathbf W_{J1}^{*T}\left(\phi_{J1}\phi_{J1}^T+\delta_{J1}\mathbf I\right)\mathbf W_{J1}^*\\ & +\frac{\delta_{f1}}{2}\theta_{f1}^{*2}+\frac12 e_{f1}^2+\frac12\dot\Upsilon_d^2+\frac12\eta_1^2+z_1z_2.\end{aligned} \tag{54}$$

It is evident that

$$-\tilde{\mathbf W}_{c1}^T\left(\phi_{J1}\phi_{J1}^T+\delta_{J1}\mathbf I\right)\tilde{\mathbf W}_{c1}\le-\lambda_{\phi_{J1}}^{\min}\tilde{\mathbf W}_{c1}^T\tilde{\mathbf W}_{c1} \tag{55}$$

$$-\tilde{\mathbf W}_{a1}^T\left(\phi_{J1}\phi_{J1}^T+\delta_{J1}\mathbf I\right)\tilde{\mathbf W}_{a1}\le-\lambda_{\phi_{J1}}^{\min}\tilde{\mathbf W}_{a1}^T\tilde{\mathbf W}_{a1}. \tag{56}$$

where $\lambda_{\phi_{J1}}^{\min}$ is the minimum eigenvalue of $\phi_{J1}\phi_{J1}^T+\delta_{J1}\mathbf I$. By using (55) and (56), (54) becomes

$$\begin{aligned}\dot V_1 \le & -r_{11}z_1^{2p}-(r_{12}-\frac74)z_1^2-\frac{\delta_{f1}}{2}\tilde\theta_{f1}^2-\left(\frac{\gamma_{c1}}{2}-\frac14\delta_z^2\right)\lambda_{\phi_{J1}}^{\min}\tilde{\mathbf W}_{c1}^T\tilde{\mathbf W}_{c1}-\left(\frac{\gamma_{c1}}{2}-\frac14\sigma_{z1}^2\right)\lambda_{\phi_{J1}}^{\min}\tilde{\mathbf W}_{a1}^T\tilde{\mathbf W}_{a1}\\ & +\left(\frac{\gamma_{c1}}{2}+\frac{\gamma_{a1}}{2}\right)\mathbf W_{J1}^{*T}\left(\phi_{J1}\phi_{J1}^T+\delta_{J1}\mathbf I\right)\mathbf W_{J1}^*+\frac{\delta_{f1}}{2}\theta_{f1}^{*2}+\frac12 e_{f1}^2+\frac12\dot\Upsilon_d^2+\frac12\eta_1^2+z_1z_2\end{aligned} \tag{57}$$

where the design constants must satisfy $r_{12}>7/4$ and $\gamma_{a1}>\gamma_{c1}>\max(\gamma_{a1}/2,\delta_{z1}^2/2)$.

Step *i* ($\mathbf{2\le i\le n}-1$): Define $z_i:=\xi_i-\hat\alpha_{i-1}^*$. According to the transformed system, the dynamic equation can be obtained as

$$\dot z_i=\dot\xi_i-\dot{\hat\alpha}_{i-1}^*=z_{i+1}+\alpha_i+\mathfrak{F}_i^\sigma\left(\bar{\boldsymbol\xi}_{i+1}\right)-\dot{\hat\alpha}_{i-1}^*. \tag{58}$$

For optimization, the value function is defined as:

$$J_i^*:=\min_{\alpha_i}\left(\int_t^\infty h_i\left(z_i(s),\alpha_i(s)ds\right)\right)=\int_t^\infty h_i\left(z_i(s),\alpha_i^*(s)ds\right) \tag{59}$$

where $h_i(z_i,\alpha_i)=z_i^2+\alpha_i^2$ is the local cost function, α_i is the virtual controller, and α_i^* is its optimal value. Using (59), the HJB equation is expressed as follows:

$$H_i(z_i,\alpha_i^*,\frac{dJ_i^*}{dz_i})=h_i(z_i,\alpha_i^*)+\frac{dJ_i^*(z_i)}{dz_i}\dot z_i=z_i^2+\alpha_i^{*2}+\frac{dJ_i^*(z_i)}{dz_i}\left(z_{i+1}+\alpha_i^*+\mathfrak{F}_i^\sigma\left(\bar{\boldsymbol\xi}_{i+1}\right)-\dot{\hat\alpha}_{i-1}^*\right). \tag{60}$$

From (60), the optimal virtual controller can be written as

$$\alpha_i^*=-\frac12\frac{dJ_i^*(z_i)}{dz_i}. \tag{61}$$

By substituting (61) into (60), the HJB equation becomes

$$z_i^2+\left(\frac{1}{2}\frac{dJ_i^*(z_i)}{dz_i}\right)^2\left(z_i-\frac{1}{2}\frac{dJ_i^*(z_i)}{dz_i}+\mathfrak{F}_i^{\sigma}\left(\bar{\xi}_{i+1}\right)-\dot{\alpha}_{i-1}^*\right)=0\,. \tag{62}$$

Solving the nonlinear differential equation in (62) is nontrivial. To address this challenge, an identifier-actor-critic NN, similar to step 1, is constructed as follows:

$$F_i^{\sigma}\left(\bar{\boldsymbol{\xi}}_{\mathbf{i+1}},\dot{\alpha}_{i-1},z_{i-1}\right)=\mathfrak{F}_i^{\sigma}\left(\bar{\xi}_{i+1}\right)-\dot{\alpha}_{i-1}^*+z_{i-1} \tag{63}$$

$$\boldsymbol{\phi}_{fi}=\boldsymbol{\phi}_f\left(\mathbf{X}_{fi}\right) \tag{64}$$

$$F_i^{\sigma}\left(\mathbf{X}_{fi}\right)=\mathbf{W}_{fi}^{*\sigma T}\boldsymbol{\phi}_f\left(\mathbf{X}_{fi}\right)+\varepsilon_{fi}^{\sigma},\quad \left|\varepsilon_{fi}^{\sigma}\right|<e_{fi} \tag{65}$$

where $\mathbf{W}_{fi}^{*\sigma T}$ is the vector ideal weights of the network. $\varepsilon_{fi}^{\sigma}$ is the approximation error and e_{fi} is its upper bound. The input to this network is $\mathbf{X}_{fi}=\left(\bar{\boldsymbol{\xi}}_{\mathbf{i+1}},z_1,...,z_{i-1},\theta_{f1},...,\theta_{f(i-1)},\mathbf{W}_{a1},...,\mathbf{W}_{a(i-1)}\right)$ in which θ_{fi} is the estimation of $\theta_{fi}^*=\max\{\|\mathbf{W}_{fi}^{*\sigma}\|\}$. Similar to (30), an actor–critic NN is formulated as follows:

$$\frac{d\hat{J}_i^*}{dz_i}=2r_{i1}z_i^{2p-1}+2r_{i2}z_i+\mathbf{W}_{ci}^T\boldsymbol{\phi}_{Ji}+\frac{1}{\eta_i^2}z_i\theta_{fi}\boldsymbol{\phi}_{fi}^T\boldsymbol{\phi}_{fi} \tag{66}$$

$$\hat{\alpha}_i^*=-\frac{1}{2}\mathbf{W}_{ai}^T\boldsymbol{\phi}_{Ji}-r_{i1}z_i^{2p-1}-r_{i2}z_i-\frac{1}{2\eta_i^2}z_i\theta_{fi}\boldsymbol{\phi}_{fi}^T\boldsymbol{\phi}_{fi} \tag{67}$$

where $\mathbf{W}_{ai}$ and $\mathbf{W}_{ci}$ are is the actor and critic weights, respectively, r_{i1}, r_{i2} and η_i are positive design constants, and $\mathbf{X}_{Ji}=(\mathbf{X}_{fi},z_i)$. For brevity, the basis function $\boldsymbol{\phi}_J(\mathbf{X}_{Ji})$ is represented as $\boldsymbol{\phi}_{Ji}$. As a result, the HJB approximation become

$$\begin{aligned}H_i\left(z_i,\hat{\alpha}_i^*,\frac{d\hat{J}_i^*}{dz_i}\right)=z_i^2&+\left(\frac{1}{2}\mathbf{W}_{ai}^T\boldsymbol{\phi}_{Ji}+r_{i1}z_i^{2p-1}+r_{i2}z_i+\frac{1}{2\eta_i^2}z_i\theta_{fi}\boldsymbol{\phi}_{fi}^T\boldsymbol{\phi}_{fi}\right)^2\\&+\left(2r_{i1}z_i^{2p-1}+2r_{i2}z_i+\frac{1}{\eta_i^2}z_i\theta_{fi}\boldsymbol{\phi}_{fi}^T\boldsymbol{\phi}_{fi}+\mathbf{W}_{ci}^T\boldsymbol{\phi}_{Ji}\right)\\&\left(z_{i+1}-\frac{1}{2}W_{ai}^T\boldsymbol{\phi}_{Ji}-r_{i1}z_i^{2p-1}-r_{i2}z_i\right.\\&\left.-\frac{1}{2\eta_i^2}z_i\theta_{fi}\boldsymbol{\phi}_{fi}^T\boldsymbol{\phi}_{fi}+\mathbf{W}_{fi}^{*\sigma T}\boldsymbol{\phi}_{fi}-z_{i-1}+\varepsilon_{fi}^{\sigma}-\dot{\hat{\alpha}}_{i-1}^*\right).\end{aligned} \tag{68}$$

Similar to step 1, as the HJB has a unique solution, the controller must satisfy the following equation:

$$\frac{\partial H_i\left(z_i,\hat{\alpha}_i^*,\frac{d\hat{J}_i^*}{dz_i}\right)}{\partial W_{ai}}=\frac{1}{2}\boldsymbol{\phi}_{Ji}\boldsymbol{\phi}_{Ji}^T\left(\mathbf{W}_{ai}-\mathbf{W}_{ci}\right)=0\,. \tag{69}$$

To derive the actor-critic update laws that ensure (69), a positive-definite function is introduced as follows:

$$P_i(t):=\left(\mathbf{W}_{ai}-\mathbf{W}_{ci}\right)^T\left(\mathbf{W}_{ai}-\mathbf{W}_{ci}\right). \tag{70}$$

It is apparent that $P_i(t)=0$ is equal to (69). The weights of the actor and critic networks are updated according to the following laws:

$$\dot{W}_{ai}=-\frac{1}{2}\delta_i\boldsymbol{\phi}_{Ji}z_i-\left(\boldsymbol{\phi}_{Ji}\boldsymbol{\phi}_{Ji}^T+\delta_{Ji}\mathbf{I}\right)\left(\gamma_{ai}\left(\mathbf{W}_{ai}-\mathbf{W}_{ci}\right)+\gamma_{ci}\mathbf{W}_{ci}\right) \tag{71}$$

$$\dot{W}_{ci}=-\frac{1}{2}\delta_{zi}\boldsymbol{\phi}_{Ji}z_i-\gamma_{ci}\left(\boldsymbol{\phi}_{Ji}\boldsymbol{\phi}_{Ji}^T+\delta_{Ji}\mathbf{I}\right)\mathbf{W}_{ci} \tag{72}$$

where γ_{ai} and γ_{ci} are positive constants and δ_{Ji} and δ_{zi} are small positive constants. The time derivative of (70) is

$$\frac{dP_i}{dt}=-\frac{\gamma_{ai}}{2}\frac{\partial P_i}{\partial\mathbf{W}_{ai}^T}\left(\boldsymbol{\phi}_{Ji}\boldsymbol{\phi}_{Ji}^T+\delta_{Ji}\mathbf{I}\right)\frac{\partial P_i}{\partial\mathbf{W}_{ai}}\le 0\,. \tag{73}$$

Inequality (73) indicates that $P_i(t)=0$ is eventually achieved and hence $H_i(z_i,\hat{\alpha}_i^*,d\hat{J}_i^*/dz_i)\to 0$. The Lyapunov function is considered as follows:

$$V_i:=\frac{1}{2}z_i^2+\frac{1}{2}\tilde{\theta}_{fi}^2+\frac{1}{2}\tilde{\mathbf{W}}_{ai}^T\tilde{\mathbf{W}}_{ai}+\frac{1}{2}\tilde{\mathbf{W}}_{ci}^T\tilde{\mathbf{W}}_{ci}+V_{i-1} \tag{74}$$

where $\tilde{\theta}_{fi}=\theta_{fi}-\theta_{fi}^*$, $\tilde{\mathbf{W}}_{ai}=\mathbf{W}_{ai}-\mathbf{W}_{Ji}^*$, and $\tilde{\mathbf{W}}_{ci}=\mathbf{W}_{ci}-\mathbf{W}_{Ji}^*$. Using the identifier NN in (65), the virtual controller in (67), and the actor-critic update laws in (71) and (72), the derivative of (74) becomes

$$\dot{V}_i = z_i\left(z_{i+1} - \frac{1}{2}\mathbf{W}_{ai}^T\boldsymbol{\phi}_{Ji} - r_{i2}z_i - r_{i1}z_i^{2p-1}\frac{1}{2\eta_i^2}z_i\theta_{fi}\boldsymbol{\phi}_{fi}^T\boldsymbol{\phi}_{fi} + \mathbf{W}_{fi}^{*\sigma T}\boldsymbol{\phi}_{fi} + \varepsilon_{fi}^{\sigma}\right)$$
$$+\tilde{\mathbf{W}}_{ai}^T\left(-\frac{1}{2}\delta_{zi}\boldsymbol{\phi}_{Ji}z_i - \left(\boldsymbol{\phi}_{Ji}\boldsymbol{\phi}_{Ji}^T + \delta_{Ji}\mathbf{I}\right)\left(\gamma_{ai}\left(\mathbf{W}_{ai} - \mathbf{W}_{ci}\right) + \gamma_{ci}\mathbf{W}_{ci}\right)\right) \tag{75}$$
$$+\tilde{\mathbf{W}}_{ci}^T\left(-\frac{1}{2}\delta_{zi}\boldsymbol{\phi}_{Ji}z_i - \gamma_{ci}\left(\boldsymbol{\phi}_{Ji}\boldsymbol{\phi}_{Ji}^T + \delta_{Ji}\mathbf{I}\right)\mathbf{W}_{ci}\right) - z_i z_{i-1} + \tilde{\theta}_{fi}\dot{\theta}_{fi} + \dot{V}_{i-1}$$

Applying Lemma 2 gives

$$z_i\,\varepsilon_{fi}^{\sigma} \le \frac{1}{2}z_i^2 + \frac{1}{2}e_{fi}^2 \tag{76}$$

$$-\frac{1}{2}z_i\mathbf{W}_{ai}^T\boldsymbol{\phi}_{Ji} \le \frac{1}{4}z_i^2 + \frac{1}{4}\mathbf{W}_{ai}^T\left(\boldsymbol{\phi}_{Ji}\boldsymbol{\phi}_{Ji}^T + \delta_{Ji}\mathbf{I}\right)\mathbf{W}_{ai} \tag{77}$$

$$-\frac{1}{2}z_i\delta_{zi}\tilde{\mathbf{W}}_{ai}^T\boldsymbol{\phi}_{Ji} \le \frac{1}{4}z_i^2 + \frac{1}{4}\delta_{zi}^2\tilde{\mathbf{W}}_{ai}^T\left(\boldsymbol{\phi}_{Ji}\boldsymbol{\phi}_{Ji}^T + \delta_{Ji}\mathbf{I}\right)\tilde{\mathbf{W}}_{ai} \tag{78}$$

$$-\frac{1}{2}z_i\delta_{zi}\tilde{\mathbf{W}}_{ci}^T\boldsymbol{\phi}_{Ji} \le \frac{1}{4}z_i^2 + \frac{1}{4}\delta_{zi}^2\tilde{\mathbf{W}}_{ci}^T\left(\boldsymbol{\phi}_{Ji}\boldsymbol{\phi}_{Ji}^T + \delta_{Ji}\mathbf{I}\right)\tilde{\mathbf{W}}_{ci} \tag{79}$$

$$z_i\mathbf{W}_{fi}^{*\sigma T}\boldsymbol{\phi}_{fi} \le \frac{1}{2}\eta_i^2 + \frac{1}{2\eta_i^2}z_i^2\theta_{fi}^*\boldsymbol{\phi}_{fi}\boldsymbol{\phi}_{fi} \tag{80}$$

By defining the adaptation law as

$$\dot{\theta}_{fi} := \frac{1}{2\eta_i^2}z_i^2\boldsymbol{\phi}_{fi}^T\boldsymbol{\phi}_{fi} - \delta_{fi}\theta_{fi} \tag{81}$$

and applying (76)–(81), (75) can be rewritten as

$$\dot{V}_i \le -r_{i1}z_i^{2p} - (r_{i2} - \frac{5}{4})z_i^2 - \delta_{fi}\tilde{\theta}_{fi}\theta_{fi} - \gamma_{ci}\tilde{\mathbf{W}}_{ci}^T\left(\boldsymbol{\phi}_{Ji}\boldsymbol{\phi}_{Ji}^T + \delta_{Ji}\mathbf{I}\right)\mathbf{W}_{ci} - \gamma_{ai}\tilde{\mathbf{W}}_{ai}^T\left(\boldsymbol{\phi}_{Ji}\boldsymbol{\phi}_{Ji}^T + \delta_{Ji}\mathbf{I}\right)\mathbf{W}_{ai}$$
$$+(\gamma_{ai} - \gamma_{ci})\tilde{\mathbf{W}}_{ai}^T\left(\boldsymbol{\phi}_{Ji}\boldsymbol{\phi}_{Ji}^T + \delta_{Ji}\mathbf{I}\right)\mathbf{W}_{ci} + \frac{1}{4}\mathbf{W}_{ai}^T\left(\boldsymbol{\phi}_{Ji}\boldsymbol{\phi}_{Ji}^T + \delta_{Ji}\mathbf{I}\right)\mathbf{W}_{ai} + \frac{1}{4}\delta_{zi}^2\tilde{\mathbf{W}}_{ai}^T\left(\boldsymbol{\phi}_{Ji}\boldsymbol{\phi}_{Ji}^T + \delta_{Ji}\mathbf{I}\right)\tilde{\mathbf{W}}_{ai} \tag{82}$$
$$+\frac{1}{4}\delta_{zi}^2\tilde{\mathbf{W}}_{ci}^T\left(\boldsymbol{\phi}_{Ji}\boldsymbol{\phi}_{Ji}^T + \delta_{Ji}\mathbf{I}\right)\tilde{\mathbf{W}}_{ci} + \frac{1}{2}e_{fi}^2 + \frac{1}{2}\eta_i^2 + z_i z_{i+1} - z_i z_{i-1} + \dot{V}_{i-1}$$

where δ_{fi} is a positive constant. According to the definition of $\tilde{\theta}_{fi}$, $\tilde{\mathbf{W}}_{ci}$, and $\tilde{\mathbf{W}}_{ai}$, the following equations are obtained:

$$\tilde{\theta}_{fi}\theta_{fi} = \frac{1}{2}\tilde{\theta}_{fi}^2 + \frac{1}{2}\theta_{fi}^2 - \frac{1}{2}\theta_{fi}^{*2} \tag{83}$$

$$\tilde{\mathbf{W}}_{ci}^T\left(\boldsymbol{\phi}_{Ji}\boldsymbol{\phi}_{Ji}^T + \delta_{Ji}\mathbf{I}\right)\mathbf{W}_{ci} = \frac{1}{2}\tilde{\mathbf{W}}_{ci}^T\left(\boldsymbol{\phi}_{Ji}\boldsymbol{\phi}_{Ji}^T + \delta_{Ji}\mathbf{I}\right)\tilde{\mathbf{W}}_{ci} + \frac{1}{2}\mathbf{W}_{ci}^T\left(\boldsymbol{\phi}_{Ji}\boldsymbol{\phi}_{Ji}^T + \delta_{Ji}\mathbf{I}\right)\mathbf{W}_{ci} - \frac{1}{2}\mathbf{W}_{Ji}^{*T}\left(\boldsymbol{\phi}_{Ji}\boldsymbol{\phi}_{Ji}^T + \delta_{Ji}\mathbf{I}\right)\mathbf{W}_{Ji}^* \tag{84}$$

$$\tilde{\mathbf{W}}_{ai}^T\left(\boldsymbol{\phi}_{Ji}\boldsymbol{\phi}_{Ji}^T + \delta_{Ji}\mathbf{I}\right)\mathbf{W}_{ai} = \frac{1}{2}\tilde{\mathbf{W}}_{ai}^T\left(\boldsymbol{\phi}_{Ji}\boldsymbol{\phi}_{Ji}^T + \delta_{Ji}\mathbf{I}\right)\tilde{\mathbf{W}}_{ai} + \frac{1}{2}\mathbf{W}_{ai}^T\left(\boldsymbol{\phi}_{Ji}\boldsymbol{\phi}_{Ji}^T + \delta_{Ji}\mathbf{I}\right)\mathbf{W}_{ai} - \frac{1}{2}\mathbf{W}_{Ji}^{*T}\left(\boldsymbol{\phi}_{Ji}\boldsymbol{\phi}_{Ji}^T + \delta_{Ji}\mathbf{I}\right)\mathbf{W}_{Ji}^*. \tag{85}$$

Applying Lemma 2 results in

$$(\gamma_{ai} - \gamma_{ci})\tilde{\mathbf{W}}_{ai}^T\left(\boldsymbol{\phi}_{Ji}\boldsymbol{\phi}_{Ji}^T + \delta_{Ji}\mathbf{I}\right)\mathbf{W}_{ci} \le \frac{(\gamma_{ai} - \gamma_{ci})}{2}\tilde{\mathbf{W}}_{ai}^T\left(\boldsymbol{\phi}_{Ji}\boldsymbol{\phi}_{Ji}^T + \delta_{Ji}\mathbf{I}\right)\tilde{\mathbf{W}}_{ai} + \frac{(\gamma_{ai} - \gamma_{ci})}{2}\mathbf{W}_{ci}\left(\boldsymbol{\phi}_{Ji}\boldsymbol{\phi}_{Ji}^T + \delta_{Ji}\mathbf{I}\right)\mathbf{W}_{ci}. \tag{86}$$

Using (83)–(86), (82) becomes

$$\dot{V}_i \le -r_{i1}z_i^{2p} - (r_{i2} - \frac{3}{4})z_i^2 - \frac{\delta_{fi}}{2}\tilde{\theta}_{fi}^2 - \left(\frac{\gamma_{ci}}{2} - \frac{1}{4}\delta_{zi}^2\right)\tilde{\mathbf{W}}_{ci}\left(\boldsymbol{\phi}_{Ji}\boldsymbol{\phi}_{Ji}^T + \delta_{Ji}\mathbf{I}\right)\tilde{\mathbf{W}}_{ci}$$
$$-\left(\frac{\gamma_{ci}}{2} - \frac{1}{4}\delta_{zi}^2\right)\tilde{\mathbf{W}}_{ai}^T\left(\boldsymbol{\phi}_{Ji}\boldsymbol{\phi}_{Ji}^T + \delta_{Ji}\mathbf{I}\right)\tilde{\mathbf{W}}_{ai} - \left(\gamma_{ci} - \frac{\gamma_{ai}}{2}\right)\mathbf{W}_{ci}^T\left(\boldsymbol{\phi}_{Ji}\boldsymbol{\phi}_{Ji}^T + \delta_{Ji}\mathbf{I}\right)\mathbf{W}_{ci}$$
$$-\left(\frac{\gamma_{ai}}{2} - \frac{1}{4}\right)\mathbf{W}_{ai}^T\left(\boldsymbol{\phi}_{Ji}\boldsymbol{\phi}_{Ji}^T + \delta_{Ji}\mathbf{I}\right)\mathbf{W}_{ai} + \left(\frac{\gamma_{ci}}{2} + \frac{\gamma_{ai}}{2}\right)\mathbf{W}_{Ji}^{*T}\left(\boldsymbol{\phi}_{Ji}\boldsymbol{\phi}_{Ji}^T + \delta_{Ji}\mathbf{I}\right)\mathbf{W}_{Ji}^* \tag{87}$$
$$+\frac{\delta_{fi}}{2}\theta_{fi}^{*2} + \frac{1}{2}e_{fi}^2 + \frac{1}{2}\eta_i^2 + z_i z_{i+1} - z_i z_{i-1} + \dot{V}_{i-1}.$$

It is evident that

$$-\tilde{\mathbf{W}}_{ci}^T\left(\boldsymbol{\phi}_{Ji}\boldsymbol{\phi}_{Ji}^T + \delta_{Ji}\mathbf{I}\right)\tilde{\mathbf{W}}_{ci} \le -\lambda_{\boldsymbol{\phi}_{Ji}}^{\min}\tilde{\mathbf{W}}_{ci}^T\tilde{\mathbf{W}}_{ci} \tag{88}$$

$$-\tilde{\mathbf{W}}_{ai}^T\left(\boldsymbol{\phi}_{Ji}\boldsymbol{\phi}_{Ji}^T + \delta_{Ji}\mathbf{I}\right)\tilde{\mathbf{W}}_{ai} \le -\lambda_{\boldsymbol{\phi}_{Ji}}^{\min}\tilde{\mathbf{W}}_{ai}^T\tilde{\mathbf{W}}_{ai}\,. \tag{89}$$

where $\lambda_{\boldsymbol{\phi}_{Ji}}^{\min}$ is the minimum eigenvalue of $\boldsymbol{\phi}_{Ji}\boldsymbol{\phi}_{Ji}^T + \delta_{Ji}\mathbf{I}$. Using (88) and (89), (87) can be rewritten as

$$\begin{aligned}\dot{V}_i \le & -r_{i1} z_i^{2p} - (r_{i2} - \frac{5}{4}) z_i^2 - \frac{\delta_{fi}}{2}\tilde{\theta}_{fi}^2 - \left(\frac{\gamma_{ci}}{2} - \frac{1}{4}\delta_{zi}^2\right)\lambda_{\phi_{Ji}}^{\min} \tilde{\mathbf{W}}_{ci} \tilde{\mathbf{W}}_{ci} \\ & - \left(\frac{\gamma_{ci}}{2} - \frac{1}{4}\delta_{zi}^2\right)\lambda_{\phi_{Ji}}^{\min} \tilde{\mathbf{W}}_{ai}^T \tilde{\mathbf{W}}_{ai} + \left(\frac{\gamma_{ci}}{2} + \frac{\gamma_{ai}}{2}\right)\mathbf{W}_{Ji}^{*T}\left(\boldsymbol{\phi}_{Ji}\boldsymbol{\phi}_{Ji}^T + \delta_{Ji}\mathbf{I}\right)\mathbf{W}_{Ji}^* \\ & + \frac{\delta_{fi}}{2}\theta_{fi}^{*2} + \frac{1}{2}e_{fi}^2 + \frac{1}{2}\eta_i^2 + z_i z_{i+1} - z_i z_{i-1} + \dot{V}_{i-1}\end{aligned} \tag{90}$$

where the design constants must satisfy $r_{i2} > 5/4$ and $\gamma_{ai} > \gamma_{ci} > \max(\gamma_{ai}/2, \delta_{zi}^2/2)$.

Step *n*: Define $z_n := \xi_n - \hat{\alpha}_{n-1}^*$. Then, according to the transformed system, the following dynamic equation is derived:

$$\dot{z}_n = \mathfrak{F}_n^{\sigma}\left(\bar{\xi}_n\right) + \mathfrak{G}_n u - \dot{\hat{\alpha}}_{n-1}^*. \tag{91}$$

For optimization purposes, the value function is defined as

$$J_n^* := \min_{\alpha_n}\left(\int_t^{\infty} h_n\left(z_n(s), u(s)ds\right)\right) = \int_t^{\infty} h_n\left(z_n(s), u^*(s)ds\right) \tag{92}$$

where $h_n(z_n, u) = z_n^2 + u^2$ is the local cost function, u is the control signal, and u^* is its optimal value. Using (92), the HJB equation can be obtained as follows:

$$H_n(z_n, u^*, \frac{dJ_n^*}{dz_n}) = h_n(z_n, u^*) + \frac{dJ_n^*(z_n)}{dz_n}\dot{z}_n = z_n^2 + u^{*2} + \frac{dJ_n^*(z_n)}{dz_n}\left(\mathfrak{F}_n^{\sigma}(\bar{\xi}_n) - \dot{\alpha}_{n-1}^* + \mathfrak{G}_n u^*\right). \tag{93}$$

From (93), the optimal controller can be obtained as

$$u^* = -\frac{\mathfrak{G}_n}{2}\frac{dJ_n^*(z_n)}{dz_n}. \tag{94}$$

Substituting (94) in (93), the HJB equation is

$$z_n^2 + \left(\frac{\mathfrak{G}_n}{2}\frac{dJ_n^*(z_n)}{dz_n}\right)^2 + \frac{dJ_n^*(z_n)}{dz_n}\left(-\mathfrak{G}_n\frac{\mathfrak{G}_n}{2}\frac{dJ_n^*(z_n)}{dz_n} + \mathfrak{F}_n^{\sigma}\left(\bar{\xi}_n\right) - \dot{\alpha}_{n-1}^*\right) = 0. \tag{95}$$

Solving the nonlinear differential equation in (95) is a challenging task. To address this issue, an identifier-actor-critic NN, similar to the previous steps, is designed as follows:

$$F_n^{\sigma}\left(\bar{\xi}_n, \dot{\alpha}_{n-1}, z_{n-1}\right) = : \mathfrak{F}_n^{\sigma}\left(\bar{\xi}_n\right) - \dot{\hat{\alpha}}_{n-1}^* + z_{n-1} \tag{96}$$

$$\boldsymbol{\phi}_{fn} = \boldsymbol{\phi}_f\left(\mathbf{X}_{fn}\right) \tag{97}$$

$$F_n^{\sigma}\left(\mathbf{X}_{fn}\right) = \mathbf{W}_{fn}^{*\sigma T}\boldsymbol{\phi}_f\left(\mathbf{X}_{fn}\right) + \varepsilon_{fn}^{\sigma}, \quad \left|\varepsilon_{fn}^{\sigma}\right| < e_{fn} \tag{98}$$

where $\mathbf{W}_{fn}^{*\sigma T}$ is the ideal weights of the NN identifier. $\varepsilon_{fn}^{\sigma}$ is the approximation error and e_{fn} is its upper bound, The input to this network is $\mathbf{X}_{fn} = \left(\bar{\boldsymbol{\xi}}_{\mathbf{i+1}}, z_1, ..., z_{n-1}, \theta_{f1}, ..., \theta_{f(n-1)}, \mathbf{W}_{a1}, ..., \mathbf{W}_{a(n-1)}\right)$ and θ_{fn} is the estimation of $\theta_{fn}^* = \max\{\|\mathbf{W}_n^{*\sigma}\|\}$. An actor–critic NN framework is formulated as follows:

$$\frac{d\hat{J}_n^*}{dz_n} = \frac{1}{\mathfrak{G}_n^2}\left(2r_{n2}z_n + 2r_{n1}z_n^{2p-1} + \mathbf{W}_{cn}^T\boldsymbol{\phi}_{Jn} + \frac{1}{\eta_n^2}z_n\theta_{fn}\boldsymbol{\phi}_{fn}^T\boldsymbol{\phi}_{fn}\right) \tag{99}$$

$$\hat{u}^* = \frac{-1}{\mathfrak{G}_n}\left(\frac{1}{2}\mathbf{W}_{an}^T\boldsymbol{\phi}_{Jn} - r_{n2}z_n - r_{n1}z_n^{2p-1} - \frac{1}{2\eta_n^2}z_n\theta_{fn}\boldsymbol{\phi}_{fn}^T\boldsymbol{\phi}_{fn}\right) \tag{100}$$

where $\mathbf{W}_{an}$ is the actor and $\mathbf{W}_{cn}$ is the critic NN weights, $\mathbf{X}_{Jn} = (\mathbf{X}_{fn}, z_n)$, and r_{in}, r_{in} and η_n are positive design constants. For brevity, $\boldsymbol{\phi}_J(\mathbf{X}_{Jn})$ is represented as $\boldsymbol{\phi}_{Jn}$. As a result, the HJB approximation is obtained as

$$\begin{aligned}H_n(z_n, \hat{u}^*, \frac{d\hat{J}_n^*}{dz_n}) = & z_n^2 + \frac{1}{\mathfrak{G}_n^2}\left(\frac{1}{2}\mathbf{W}_{an}^T + r_{n2}z_n + r_{n1}z_n^{2p-1} + \frac{1}{2\eta_n^2}z_n\theta_{fn}\boldsymbol{\phi}_{fn}^T\boldsymbol{\phi}_{fn}\right)^2 \\ & + \frac{1}{\mathfrak{G}_n^2}\left(2r_{n2}z_n + 2r_{n1}z_n^{2p-1} + \mathbf{W}_{cn}^T\boldsymbol{\phi}_{Jn} + \frac{1}{\eta_n^2}z_n\theta_{fn}\boldsymbol{\phi}_{fn}^T\boldsymbol{\phi}_{fn}\right) \\ & \times\left(\mathbf{W}_{fn}^{*\sigma T}\boldsymbol{\phi}_f\left(\mathbf{X}_{fn}\right) + \varepsilon_{fn}^{\sigma} - z_{n-1} - \frac{1}{2}\mathbf{W}_{an}^T\boldsymbol{\phi}_{Jn} - r_{n2}z_n - r_{n1}z_n^{2p-1} - \frac{1}{2\eta_n^2}z_n\theta_{fn}\boldsymbol{\phi}_{fn}^T\boldsymbol{\phi}_{fn}\right).\end{aligned} \tag{101}$$

Similarly, since HJB has a unique solution, the controller must satisfy the following equation:

$$\frac{\partial H_n(z_n,\hat{u}^*,\frac{d\hat{J}_n^*}{dz_n})}{\partial \mathbf{W}_{an}} = \frac{1}{2\mathfrak{S}_n^2}\boldsymbol{\phi}_{Jn}\boldsymbol{\phi}_{Jn}^T\left(\mathbf{W}_{an}-\mathbf{W}_{cn}\right)=0. \tag{102}$$

To derive the actor-critic update laws that ensure (102), a positive-definite function is introduced as follows:

$$P_n(t) := \left(\mathbf{W}_{an}-\mathbf{W}_{cn}\right)^T\left(\mathbf{W}_{an}-\mathbf{W}_{cn}\right). \tag{103}$$

It is obvious that $P_n(t)=0$ is equal to (102). The actor and critic network weights are updated as follows:

$$\dot{\mathbf{W}}_{an} = -\frac{1}{2}\delta_{zn}\boldsymbol{\phi}_{Jn}z_n - \left(\boldsymbol{\phi}_{Jn}\boldsymbol{\phi}_{Jn}^T+\delta_{Jn}\mathbf{I}\right)\left(\gamma_{an}\left(\mathbf{W}_{an}-\mathbf{W}_{cn}\right)+\gamma_{cn}\mathbf{W}_{cn}\right) \tag{104}$$

$$\dot{\mathbf{W}}_{cn} = -\frac{1}{2}\delta_{zn}\boldsymbol{\phi}_{Jn}z_n - \gamma_{cn}\left(\boldsymbol{\phi}_{Jn}\boldsymbol{\phi}_{Jn}^T+\delta_{Jn}\mathbf{I}\right)\mathbf{W}_{cn} \tag{105}$$

where γ_{an} and γ_{cn} are positive constants and δ_{Jn} and δ_{zn} are small positive constants. As a result, the derivative of $P_n(t)$ is

$$\frac{dP_n}{dt} = -\frac{\gamma_{an}}{2}\frac{\partial P_n}{\partial \mathbf{W}_{an}^T}\left(\boldsymbol{\phi}_{Jn}\boldsymbol{\phi}_{Jn}^T+\delta_{Jn}\mathbf{I}\right)\frac{\partial P_n}{\partial \mathbf{W}_{an}} \le 0. \tag{106}$$

Inequality (106) means that $P_n(t)=0$ is eventually achieved and hence, $H_n(z_n,\hat{u}^*,d\hat{J}_n^*/dz_n)\to 0$ is obtained. The Lyapunov function is defined as follows:

$$V_n := \frac{1}{2}z_n^2+\frac{1}{2}\tilde{\theta}_{fn}^2+\frac{1}{2}\tilde{\mathbf{W}}_{an}{}^T\tilde{\mathbf{W}}_{an}+\frac{1}{2}\tilde{\mathbf{W}}_{cn}{}^T\tilde{\mathbf{W}}_{cn}+V_{n-1} \tag{107}$$

where $\tilde{\theta}_{fn}=\theta_{fn}-\theta_{fn}^*$, $\tilde{\mathbf{W}}_{an}=\mathbf{W}_{an}-\mathbf{W}_{Jn}^*$, and $\tilde{\mathbf{W}}_{cn}=\mathbf{W}_{cn}-\mathbf{W}_{Jn}^*$. Using the identifier NN in (98), controller in (100), and the actor-critic update laws in (104) and (105), the derivative of the Lyapunov function can be written as follows:

$$\begin{aligned}\dot{V}_n &= z_n\left(\mathbf{W}_{fn}^{*\sigma T}\boldsymbol{\phi}_{fn}+\varepsilon_{fn}{}^{\sigma}-\frac{1}{2}W_{an}^T\boldsymbol{\phi}_{Jn}-r_{n1}z_n^{2p-1}-r_{n2}z_n-\frac{1}{2\eta_n^2}z_n\theta_{fn}\boldsymbol{\phi}_{fn}^T\boldsymbol{\phi}_{fn}\right)-z_nz_{n-1}+\tilde{\theta}_{fn}\dot{\theta}_{fn}\\ &\quad+\tilde{\mathbf{W}}_{an}^T\left(-\frac{1}{2}\delta_{zn}\boldsymbol{\phi}_{Jn}z_n-\left(\boldsymbol{\phi}_{Jn}\boldsymbol{\phi}_{Jn}^T+\delta_{Jn}\mathbf{I}\right)\left(\gamma_{an}\left(\mathbf{W}_{an}-\mathbf{W}_{cn}\right)+\gamma_{cn}\mathbf{W}_{cn}\right)\right)\\ &\quad-\tilde{\mathbf{W}}_{cn}^T\left(\frac{1}{2}\delta_{zn}\boldsymbol{\phi}_{Jn}z_n+\gamma_{cn}\left(\boldsymbol{\phi}_{Jn}\boldsymbol{\phi}_{Jn}^T+\delta_{Jn}\mathbf{I}\right)\mathbf{W}_{cn}\right)+\dot{V}_{n-1}.\end{aligned} \tag{108}$$

Applying Lemma 2 yields

$$z_n\varepsilon_{fn}^{\sigma} \le \frac{1}{2}z_n^2+\frac{1}{2}e_{fn}^2 \tag{109}$$

$$-\frac{1}{2}z_n\mathbf{W}_{an}^T\boldsymbol{\phi}_{Jn} \le \frac{1}{4}z_n^2+\frac{1}{4}\mathbf{W}_{an}^T\left(\boldsymbol{\phi}_{Jn}\boldsymbol{\phi}_{Jn}^T+\delta_{Jn}\mathbf{I}\right)\mathbf{W}_{an} \tag{110}$$

$$-\frac{1}{2}z_n\delta_{zn}\tilde{\mathbf{W}}_{an}^T\boldsymbol{\phi}_{Jn} \le \frac{1}{4}z_n^2+\frac{1}{4}\sigma_{zn}^2\tilde{\mathbf{W}}_{an}^T\left(\boldsymbol{\phi}_{Jn}\boldsymbol{\phi}_{Jn}^T+\delta_{Jn}\mathbf{I}\right)\tilde{\mathbf{W}}_{an} \tag{111}$$

$$-\frac{1}{2}z_n\delta_{zn}\tilde{\mathbf{W}}_{cn}^T\boldsymbol{\phi}_{Jn} \le \frac{1}{4}z_n^2+\frac{1}{4}\delta_{zn}^2\tilde{\mathbf{W}}_{cn}^T\left(\boldsymbol{\phi}_{Jn}\boldsymbol{\phi}_{Jn}^T+\delta_{Jn}\mathbf{I}\right)\tilde{\mathbf{W}}_{cn} \tag{112}$$

$$z_n\mathbf{W}_{fn}^{*\sigma T}\boldsymbol{\phi}_{fn} \le \frac{1}{2}\eta_n^2+\frac{1}{2\eta_n^2}z_n^2\theta_{fn}^*\boldsymbol{\phi}_{fn}^T\boldsymbol{\phi}_{fn}. \tag{113}$$

By defining the adaptation law as

$$\dot{\theta}_{fn} := \frac{1}{2\eta_n^2}z_n^2\boldsymbol{\phi}_{fn}^T\boldsymbol{\phi}_{fn}-\delta_{fn}\theta_{fn} \tag{114}$$

and by using (109)–(114), (108) becomes

$$\begin{aligned}\dot{V}_n &\le -r_{n1}z_n^{2p}-(r_{n2}-\frac{5}{4})z_n^2-\delta_{fn}\tilde{\theta}_{fn}\theta_{fn}-\gamma_{cn}\tilde{\mathbf{W}}_{cn}^T\left(\boldsymbol{\phi}_{Jn}\boldsymbol{\phi}_{Jn}^T+\delta_{Jn}\mathbf{I}\right)\mathbf{W}_{cn}\\ &\quad-\gamma_{an}\tilde{\mathbf{W}}_{an}^T\left(\boldsymbol{\phi}_{Jn}\boldsymbol{\phi}_{Jn}^T+\delta_{Jn}\mathbf{I}\right)\mathbf{W}_{an}+(\gamma_{an}-\gamma_{cn})\tilde{\mathbf{W}}_{an}^T\left(\boldsymbol{\phi}_{Jn}\boldsymbol{\phi}_{Jn}^T+\delta_{Jn}\mathbf{I}\right)\mathbf{W}_{cn}\\ &\quad+\frac{1}{4}\mathbf{W}_{an}^T\left(\boldsymbol{\phi}_{Jn}\boldsymbol{\phi}_{Jn}^T+\delta_{Jn}\mathbf{I}\right)\mathbf{W}_{an}+\frac{1}{4}\delta_{zn}^2\tilde{\mathbf{W}}_{an}^T\left(\boldsymbol{\phi}_{Jn}\boldsymbol{\phi}_{Jn}^T+\delta_{Jn}\mathbf{I}\right)\tilde{\mathbf{W}}_{an}\\ &\quad+\frac{1}{4}\delta_{zn}^2\tilde{\mathbf{W}}_{cn}^T\left(\boldsymbol{\phi}_{Jn}\boldsymbol{\phi}_{Jn}^T+\delta_{Jn}\mathbf{I}\right)+\frac{1}{2}e_{fn}^2+\frac{1}{2}\eta_n^2-z_nz_{n-1}+\dot{V}_{n-1}\end{aligned} \tag{115}$$

where δ_{fn} is a positive constant. Using the definition of $\tilde{\theta}_{fn}$, $\tilde{\mathbf{W}}_{cn}$, and $\tilde{\mathbf{W}}_{an}$ the following equations are obtained:

$$\tilde{\theta}_{fn}\theta_{fn} = \frac{1}{2}\tilde{\theta}_{fn}^2 + \frac{1}{2}\theta_{fn}^2 - \frac{1}{2}\theta_{fn}^{*2} \tag{116}$$

$$\tilde{\mathbf{W}}_{cn}^T\left(\boldsymbol{\phi}_{Jn}\boldsymbol{\phi}_{Jn}^T + \delta_{Jn}\mathbf{I}\right)\mathbf{W}_{cn} = \frac{1}{2}\tilde{\mathbf{W}}_{cn}^T\left(\boldsymbol{\phi}_{Jn}\boldsymbol{\phi}_{Jn}^T + \delta_{Jn}\mathbf{I}\right)\tilde{\mathbf{W}}_{cn} + \frac{1}{2}\mathbf{W}_{cn}^T\left(\boldsymbol{\phi}_{Jn}\boldsymbol{\phi}_{Jn}^T + \delta_{Jn}\mathbf{I}\right)\mathbf{W}_{cn} - \frac{1}{2}\mathbf{W}_{Jn}^{*T}\left(\boldsymbol{\phi}_{Jn}\boldsymbol{\phi}_{Jn}^T + \delta_{Jn}\mathbf{I}\right)\mathbf{W}_{Jn}^* \tag{117}$$

$$\tilde{\mathbf{W}}_{an}^T\left(\boldsymbol{\phi}_{Jn}\boldsymbol{\phi}_{Jn}^T + \delta_{Jn}\mathbf{I}\right)\mathbf{W}_{an} = \frac{1}{2}\tilde{\mathbf{W}}_{an}^T\left(\boldsymbol{\phi}_{Jn}\boldsymbol{\phi}_{Jn}^T + \delta_{Jn}\mathbf{I}\right)\tilde{\mathbf{W}}_{an} + \frac{1}{2}\mathbf{W}_{an}^T\left(\boldsymbol{\phi}_{Jn}\boldsymbol{\phi}_{Jn}^T + \delta_{Jn}\mathbf{I}\right)\mathbf{W}_{an} - \frac{1}{2}\mathbf{W}_{Jn}^{*T}\left(\boldsymbol{\phi}_{Jn}\boldsymbol{\phi}_{Jn}^T + \delta_{Jn}\mathbf{I}\right)\mathbf{W}_{Jn}^*. \tag{118}$$

Applying Lemma 2, results in

$$(\gamma_{an} - \gamma_{cn})\tilde{\mathbf{W}}_{an}^T\boldsymbol{\phi}_{Jn}\boldsymbol{\phi}_{Jn}^T\mathbf{W}_{cn} \le \frac{(\gamma_{an} - \gamma_{cn})}{2}\tilde{\mathbf{W}}_{an}^T\left(\boldsymbol{\phi}_{Jn}\boldsymbol{\phi}_{Jn}^T + \delta_{Jn}\mathbf{I}\right)\tilde{\mathbf{W}}_{an} + \frac{(\gamma_{an} - \gamma_{cn})}{2}\mathbf{W}_{cn}\left(\boldsymbol{\phi}_{Jn}\boldsymbol{\phi}_{Jn}^T + \delta_{Jn}\mathbf{I}\right)\mathbf{W}_{cn}. \tag{119}$$

Substituting (116)–(119) in (115) gives

$$\begin{aligned}\dot{V}_n \le & -r_{n1}z_n^{2p} - (r_{n2} - \frac{5}{4})z_n^2 - \frac{\delta_{fn}}{2}\tilde{\theta}_{fn}^2 - \left(\frac{\gamma_{cn}}{2} - \frac{1}{4}\delta_{zn}^2\right)\tilde{\mathbf{W}}_{cn}\left(\boldsymbol{\phi}_{Jn}\boldsymbol{\phi}_{Jn}^T + \delta_{Jn}\mathbf{I}\right)\tilde{\mathbf{W}}_{cn} \\ & -\left(\frac{\gamma_{cn}}{2} - \frac{1}{4}\delta_{zn}^2\right)\tilde{\mathbf{W}}_{an}^T\left(\boldsymbol{\phi}_{Jn}\boldsymbol{\phi}_{Jn}^T + \delta_{Jn}\mathbf{I}\right)\tilde{\mathbf{W}}_{an} - \left(\gamma_{cn} - \frac{\gamma_{an}}{2}\right)\mathbf{W}_{cn}^T\left(\boldsymbol{\phi}_{Jn}\boldsymbol{\phi}_{Jn}^T + \delta_{Jn}\mathbf{I}\right)\mathbf{W}_{cn} \\ & -\left(\frac{\gamma_{an}}{2} - \frac{1}{4}\right)\mathbf{W}_{an}^T\left(\boldsymbol{\phi}_{Jn}\boldsymbol{\phi}_{Jn}^T + \delta_{Jn}\mathbf{I}\right)\mathbf{W}_{an} + \left(\frac{\gamma_{cn}}{2} + \frac{\gamma_{an}}{2}\right)\mathbf{W}_{Jn}^{*T}\left(\boldsymbol{\phi}_{Jn}\boldsymbol{\phi}_{Jn}^T + \delta_{Jn}\mathbf{I}\right)\mathbf{W}_{Jn}^* \\ & + \frac{\delta_{fn}}{2}\theta_{fn}^{*2} + \frac{1}{2}e_{fn}^2 + \frac{1}{2}\eta_n^2 - z_n z_{n-1} + \dot{V}_{n-1}.\end{aligned} \tag{120}$$

It is clear that

$$-\tilde{\mathbf{W}}_{cn}^T\left(\boldsymbol{\phi}_{Jn}\boldsymbol{\phi}_{Jn}^T + \delta_{Jn}\mathbf{I}\right)\tilde{\mathbf{W}}_{cn} \le -\lambda_{\phi_{Jn}}^{\min}\tilde{\mathbf{W}}_{cn}^T\tilde{\mathbf{W}}_{cn} \tag{121}$$

$$-\tilde{\mathbf{W}}_{an}^T\left(\boldsymbol{\phi}_{Jn}\boldsymbol{\phi}_{Jn}^T + \delta_{Jn}\mathbf{I}\right)\tilde{\mathbf{W}}_{an} \le -\lambda_{\phi_{Jn}}^{\min}\tilde{\mathbf{W}}_{an}^T\tilde{\mathbf{W}}_{an}. \tag{122}$$

where $\lambda_{\phi_{Jn}}^{\min}$ is the minimum eigenvalue of $\boldsymbol{\phi}_{Jn}\boldsymbol{\phi}_{Jn}^T + \delta_{Jn}\mathbf{I}$. Using (121)–(122), (120) can be simplified as

$$\begin{aligned}\dot{V}_n \le & -r_{n1}z_n^{2p} - (r_{n2} - \frac{5}{4})z_n^2 - \frac{\delta_{fn}}{2}\tilde{\theta}_{fn}^2 - \left(\frac{\gamma_{cn}}{2} - \frac{1}{4}\delta_z^2\right)\lambda_{\phi_{Jn}}^{\min}\tilde{\mathbf{W}}_{cn}\tilde{\mathbf{W}}_{cn} \\ & -\left(\frac{\gamma_{cn}}{2} - \frac{1}{4}\delta_{zn}^2\right)\lambda_{\phi_{Jn}}^{\min}\tilde{\mathbf{W}}_{an}^T\tilde{\mathbf{W}}_{an} + \left(\frac{\gamma_{cn}}{2} + \frac{\gamma_{an}}{2}\right)\mathbf{W}_{Jn}^{*T}\left(\boldsymbol{\phi}_{Jn}\boldsymbol{\phi}_{Jn}^T + \delta_{Jn}\mathbf{I}\right)\mathbf{W}_{Jn}^* \\ & + \frac{\delta_{fn}}{2}\theta_{fn}^{*2} + \frac{1}{2}e_{fn}^2 + \frac{1}{2}\eta_n^2 - z_n z_{n-1} + \dot{V}_{n-1}\end{aligned} \tag{123}$$

where the design constants must satisfy $r_{n2} > 5/4$ and $\gamma_{an} > \gamma_{cn} > \max(\gamma_{an}/2,\ \delta_{zn}^2/2)$.

Substituting (57) and (90) in (123), yields

$$\begin{aligned}\dot{V}_n \le & -\sum_{j=1}^{n} r_{j1}z_j^{2p} - (r_{12} - \frac{7}{4})z_1^2 - \sum_{j=2}^{n}(r_{j2} - \frac{5}{4})z_j^2 \quad - \sum_{j=1}^{n}\lambda_{\phi_{Jj}}^{\min}\left(\frac{\gamma_{cj}}{2} - \frac{1}{4}\delta_{zj}^2\right)\left(\tilde{\mathbf{W}}_{cj}\tilde{\mathbf{W}}_{cj} + \tilde{\mathbf{W}}_{aj}\tilde{\mathbf{W}}_{aj}\right) \\ & + \sum_{j=1}^{n}\left(\frac{\gamma_{cj}}{2} + \frac{\gamma_{aj}}{2}\right)\left(\mathbf{W}_{Jn}^{*T}\left(\boldsymbol{\phi}_{Jn}\boldsymbol{\phi}_{Jn}^T + \delta_{Jn}\mathbf{I}\right)\mathbf{W}_{Jn}^*\right) + \sum_{j=1}^{n}\frac{\delta_{fj}}{2}\tilde{\theta}_{fj}^2 + \sum_{j=1}^{n}\left(\frac{\delta_{fj}}{2}\theta_{fj}^{*2} + \frac{1}{2}e_{fj}^2 + \frac{1}{2}\eta_j^2\right).\end{aligned} \tag{124}$$

By expanding (124), the following expression is derived:

$$\begin{aligned}\dot{V}_n \le & -\sum_{j=1}^{n} r_{j1}z_j^{2p} - r_1\sum_{j=1}^{n}\left(\tilde{\mathbf{W}}_{cn}^T\tilde{\mathbf{W}}_{cn}\right)^p + r_1\sum_{j=1}^{n}\left(\tilde{\mathbf{W}}_{cn}^T\tilde{\mathbf{W}}_{cn}\right)^p - r_1\sum_{j=1}^{n}\left(\tilde{\mathbf{W}}_{an}^T\tilde{\mathbf{W}}_{an}\right)^p \\ & + r_1\sum_{j=1}^{n}\left(\tilde{\mathbf{W}}_{an}^T\tilde{\mathbf{W}}_{an}\right)^p - r_1\sum_{j=1}^{n}\left(\tilde{\theta}_{fj}^2\right)^p + r_1\sum_{j=1}^{n}\left(\tilde{\theta}_{fj}^2\right)^p - (r_{12} - \frac{7}{4})z_j^2 - \sum_{j=2}^{n}(r_{j2} - \frac{5}{4})z_j^2 \\ & -\sum_{j=1}^{n}\frac{\delta_{fj}}{2}\tilde{\theta}_{fj}^2 - \sum_{j=1}^{n}\lambda_{\phi_{Ji}}^{\min}\left(\frac{\gamma_{cj}}{2} - \frac{1}{4}\delta_{zi}^2\right)\tilde{\mathbf{W}}_{cj}\tilde{\mathbf{W}}_{cj} - \sum_{j=1}^{n}\lambda_{\phi_{J}i}^{\min}\left(\frac{\gamma_{cj}}{2} - \frac{1}{4}\delta_{zi}^2\right)\tilde{\mathbf{W}}_{aj}\tilde{\mathbf{W}}_{aj} \\ & + \sum_{j=1}^{n}\left(\frac{\gamma_{cj}}{2} + \frac{\gamma_{aj}}{2}\right)\left(\mathbf{W}_{Jj}^{*T}\left(\boldsymbol{\phi}_{Jj}\boldsymbol{\phi}_{Jj}^T + \delta_{Ji}\mathbf{I}\right)\mathbf{W}_{Jj}^*\right) + \sum_{j=1}^{n}\left(\frac{\delta_{fj}}{2}\theta_{fj}^{*2} + \frac{1}{2}e_{fj}^2 + \frac{1}{2}\eta_j^2\right).\end{aligned} \tag{125}$$

Using Lemma 3 with $\nu_1 = 1$, $\nu_2 = (\sum_{j1}^{n}\tilde{\theta}_j^2)$, $\iota_1 = p$, $\iota_2 = 1 - p$ and $\iota_3 = (1-p)^{(1-p)/p}$, one can get

$$r_1\left(\sum_{j=1}^{n}\tilde{\theta}_j^2\right)^p \le r_1(1-p)^{\frac{p}{1-p}}p + r_1\sum_{j=1}^{n}\tilde{\theta}_j^2. \tag{126}$$

Similar inequalities can be obtained for $\tilde{\mathbf{W}}_{aj}$ and $\tilde{\mathbf{W}}_{cj}$ as

$$r_1\left(\sum_{j=1}^{n}\tilde{\mathbf{W}}_{cj}^T\tilde{\mathbf{W}}_{cj}\right)^p \le r_1(1-p)^{\frac{p}{1-p}}\,p + r_1\sum_{j=1}^{n}\tilde{\mathbf{W}}_{cj}^T\tilde{\mathbf{W}}_{cj} \tag{127}$$

$$r_1\left(\sum_{j=1}^{n}\tilde{\mathbf{W}}_{aj}^T\tilde{\mathbf{W}}_{aj}\right)^p \le r_1(1-p)^{\frac{p}{1-p}}\,p + r_1\sum_{j=1}^{n}\tilde{\mathbf{W}}_{aj}^T\tilde{\mathbf{W}}_{aj}. \tag{128}$$

Using (126)–(128) in (125), yields

$$\begin{aligned}\dot{V}_n \le& -\sum_{j=1}^{n} r_{j1} z_j^{2p} - r_1\sum_{j=1}^{n}\left(\tilde{\mathbf{W}}_{cj}^T\tilde{\mathbf{W}}_{cj}\right)^p - r_1\sum_{j=1}^{n}\left(\tilde{\mathbf{W}}_{aj}^T\tilde{\mathbf{W}}_{aj}\right)^p - r_1\sum_{j=1}^{n}\left(\tilde{\theta}_{fj}^2\right)^p\\
&-(r_{12}-\frac{7}{4})z_1^2 - \sum_{j=2}^{n}(r_{j2}-\frac{5}{4})z_j^2\sum_{j=1}^{n}\left(\frac{\delta_{fj}}{2}-r_1\right)\tilde{\theta}_{fj}^2 - \sum_{j=1}^{n}\left(\lambda_{\phi_{Jj}}^{\min}\left(\frac{\gamma_{cj}}{2}-\frac{1}{4}\delta_{zj}^2\right)-r_1\right)\tilde{\mathbf{W}}_{cj}\tilde{\mathbf{W}}_{cj}\\
&-\sum_{j=1}^{n}\left(\lambda_{\phi_J}^{\min}\left(\frac{\gamma_{cj}}{2}-\frac{1}{4}\delta_{zj}^2\right)-r_1\right)\tilde{\mathbf{W}}_{aj}\tilde{\mathbf{W}}_{aj} + \sum_{j=1}^{n}\left(\frac{\gamma_{cj}}{2}+\frac{\gamma_{aj}}{2}\right)\left(\mathbf{W}_{Jj}^{*T}\left(\boldsymbol{\phi}_{Jj}\boldsymbol{\phi}_{Jj}^T+\delta_{Jj}\mathbf{I}\right)\mathbf{W}_{Jj}^*\right)\\
&+\sum_{j=1}^{n}\left(\frac{\delta_{fj}}{2}\theta_{fj}^{*2}+\frac{1}{2}e_{fj}^2+\frac{1}{2}\eta_j^2\right)+3r_1(1-p)^{\frac{p}{1-p}}\,p.\end{aligned} \tag{129}$$

Considering $r_1 \le \min(\delta_{fj}/2, \lambda_{\phi_{Ji}}^{\min}(\gamma_{cj}/2-\delta_{zi}^2/4))$ and by defining

$$\rho_1 := \min\left(r_{j1}, r_1\right),$$

$$\rho_2 := \min\left(r_{12}-\frac{7}{4}, r_{j2}-\frac{5}{4}, \frac{\delta_{fj}}{2}-r_1, \lambda_{\phi_{Jj}}^{\min}\left(\frac{\gamma_{cj}}{2}-\frac{1}{4}\delta_{zj}^2\right)-r_1\right)$$

$$\rho_3 := \sum_{j=1}^{n}\left(\frac{\gamma_{cj}}{2}+\frac{\gamma_{aj}}{2}\right)\left(\mathbf{W}_{Jj}^{*T}\left(\boldsymbol{\phi}_{Jj}\boldsymbol{\phi}_{Jj}^T+\delta_J\mathbf{I}\right)\mathbf{W}_{Jnj}^*\right)+\sum_{j=1}^{n}\left(\frac{\delta_{fj}}{2}\theta_{fj}^{*2}+\frac{1}{2}e_{fj}^2+\frac{1}{2}\eta_j^2\right)+3r_1(1-p)^{\frac{p}{1-p}}\,p$$

the following equation is obtained:

$$\dot{V}_n \le -\rho_1 V_n^p - \rho_2 V_n + \rho_3. \tag{130}$$

Theorem: Consider the strict-feedback switched system in (1), with bounded initial states and reference signal. Using the actual controller in (100) and the virtual controllers in (31) and (67), and the adaptive laws in (48), (81), and (114), together with identifier NNs in (37), (71), and (104) as actor NNs, and (38), (72) and (105) as critic NNs. if Assumptions 1 and 2 hold and the design parameters satisfy the following conditions:

$$\begin{aligned}&r_{12} > 7/4, \quad \gamma_{a1} > \gamma_{c1} > \max\left(\gamma_{a1}/2, \delta_{z1}^2/2\right)\\
&r_{i2} > 5/4, \quad \gamma_{ai} > \gamma_{ci} > \max\left(\gamma_{ai}/2, \delta_{zi}^2/2\right)\\
&r_{n2} > 5/4, \quad \gamma_{an} > \gamma_{cn} > \max\left(\gamma_{an}/2, \delta_{zn}^2/2\right)\end{aligned}$$

then, the optimized control scheme ensures that all the closed-loop signals remain finite-time bounded under arbitrary switching, all constraints are satisfied, and the tracking error converges to a small neighborhood of the origin.

Proof: It can be observed from (130) that $\dot{V}_n$ can be written as

$$\dot{V}_n \le -\rho_1 V_n^p - \lambda\rho_2 V_n - (1-\lambda)\rho_2 V_n + \rho_3 \tag{131}$$

or

$$\dot{V}_n \le -\lambda\rho_1 V_n^p - (1-\lambda)\rho_1 V_n^p - \rho_2 V_n + \rho_3 \tag{132}$$

where $0<\lambda<1$. According to (131), if $V_n \ge \rho_3/(1-\lambda)\rho_2$, then $\dot{V}_n \le -\rho_1 V_n^p - \lambda\rho_2 V_n$. From Lemma 4, it can be concluded that decreasing V_n, drives $\tilde{\theta}_i$, $\tilde{\mathbf{W}}_{ai}$, $\tilde{\mathbf{W}}_{ci}$, and $z_i\,(i=1,\ldots,n)$ to the following region:

$$\tilde{\theta}_i, \tilde{\mathbf{W}}_{ai}, \tilde{\mathbf{W}}_{ci}, z_i \in \left\{V_n \le \frac{\rho_3}{(1-\lambda)\rho_2}\right\}. \tag{133}$$

Hence, the settling time is as follows:

$$T_{f1} \le \frac{1}{\lambda\rho_2(1-p)}\ln\frac{\lambda\rho_2 V^{1-p}(0)+\rho_1}{\rho_1}. \tag{134}$$

Similarly, (132) leads to

$$\tilde{\theta}_i, \tilde{\mathbf{W}}_{ai}, \tilde{\mathbf{W}}_{ci}, z_i \in \left\{ V_n \le \left(\frac{\rho_3}{(1-\lambda)\rho_1} \right)^{1/p} \right\}. \tag{135}$$

And the settling time is

$$T_{f\,2} \le \frac{1}{\rho_2(1-p)} \ln \frac{\rho_2 V^{1-p}(0) + \lambda\rho_1}{\lambda\rho_1}. \tag{136}$$

Consequently, it follows that $|z_i| \le \min\{(\rho_3/(1-\lambda)\rho_2)^{1/2}, (\rho_3/(1-\lambda)\rho_1)^{1/2p}\}$ reaches in finite time $T_f = \max\{T_{f1}, T_{f2}\}$. Similarly, it can be concluded that $\tilde{\theta}_i$, $\tilde{\mathbf{W}}_{ai}$, and $\tilde{\mathbf{W}}_{ci}$ are bounded. Since $\tilde{\theta}_i = \theta_i - \theta_i^*$, $\tilde{\mathbf{W}}_{ai} = \mathbf{W}_{ai} - \mathbf{W}_{Ji}^*$, and $\tilde{\mathbf{W}}_{ci} = \mathbf{W}_{ci} - \mathbf{W}_{Ji}^*$, it follows that θ_i, $\mathbf{W}_{ai}$, and $\mathbf{W}_{ci}$ are also bounded. Moreover, based on (31) and (67), the virtual controllers are bounded too. As $\hat{\alpha}_i^*$ and z_i are bounded, the transformed states (ξ_i) remain bounded as well. Based on (14) and the boundedness of ξ_i, the original system states are also bounded. Finally, based on (13), the boundedness of z_i $(i = 1, 2, \ldots n)$ guarantee that constraints are satisfied.

■

Corollary: The tracking error of the original system can be expressed as

$$y - y_d \le (\bar{c}_1 + \underline{c}_1) e^{\xi_1} e^{-\lambda_1 z_1} |z_1| \tag{137}$$

Proof: Based on (14), the tracking error can be written as

$$\begin{aligned} y - y_d &= \frac{\bar{c}_1 + \underline{c}_1}{e^{\Upsilon_d} + 1} - \frac{\bar{c}_1 + \underline{c}_1}{e^{\xi_1} + 1} = \frac{(\bar{c}_1 + \underline{c}_1) e^{\xi_1} (1 - e^{-z_1})}{(e^{\xi_1 - z} + 1)(e^{\xi_1} + 1)} \\ &\le (\bar{c}_1 + \underline{c}_1) e^{\xi_1} (1 - e^{-z_1}). \end{aligned} \tag{138}$$

Using the mean value theorem, $1 - e^{-z_1}$ can be written as $z_1 e^{-\lambda_1 z_1}$ with $\lambda_1 \in (0,1)$. Then, based on Theorem, z_1 is bounded. Therefore,

$$y - y_d \le (\bar{c}_1 + \underline{c}_1) e^{\xi_1} e^{-\lambda_1 z_1} |z_1|. \tag{139}$$

■

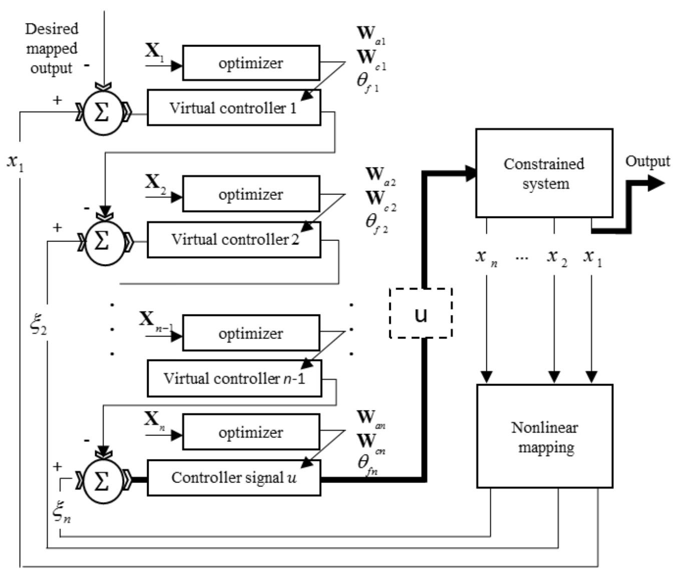

Fig. 1. Block diagram of the proposed Controller.

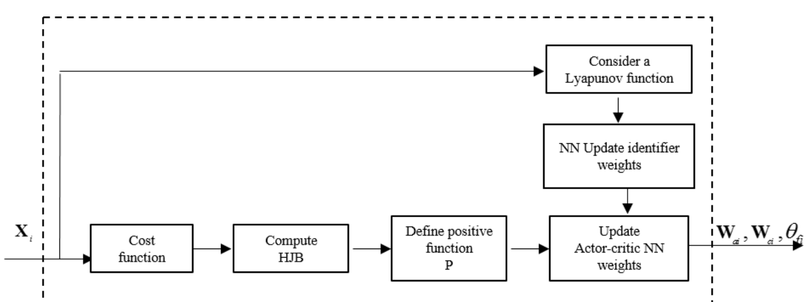

Fig. 2. Block diagram of the optimizer.

Remark 4: Since the control signal of the original system is identical to the control signal applied to the mapped system, and based on the error relationship between the original and mapped systems, it can be concluded that the optimal control signal designed for the mapped system is also optimal for the original system.

In this paper, an adaptive NN-based control scheme is developed for uncertain switched nonlinear systems subject to asymmetric time-varying constraints, using a backstepping approach. This method eliminates the feasibility condition that typically is imposed on the virtual controllers. The nonlinear terms are approximated using RBFNNs, while both the virtual and the actual controllers are optimized through actor–critic NNs. The algorithm, the block diagram of the control method, and the block diagram of the optimization structure are presented in Table I, Fig. 1, and Fig. 2 respectively.

Table I: Algorithm of the proposed method

1. Initialize θ_j, $\mathbf{W}_{aj}$, $\mathbf{W}_{cj}$ and $x_j(0)$, $j=1,\ldots,n$
2. Define constraints for system states
3. Define parameters such that

$$\begin{aligned}&r_{12}>7/4,\quad \gamma_{a1}>\gamma_{c1}>\max\left(\gamma_{a1}/2,\sigma_{z1}^2/2\right)\\&r_{j2}>5/4,\quad \gamma_{aj}>\gamma_{cj}>\max\left(\gamma_{aj}/2,\sigma_{zj}^2/2\right)\\&r_{n2}>5/4,\quad \gamma_{an}>\gamma_{cn}>\max\left(\gamma_{an}/2,\sigma_{zn}^2/2\right)\end{aligned}$$

4. Calculate the transformed states
5. Calculate virtual controller for states 1 to $n-1$ using (31) and (67)
6. Calculate controller signal using (100)
7. Update identifier NN weights θ_j using (48), (81) and (113)
8. Update actor NN weights using (37), (71) and (104)
9. Update critic NN weights using (38), (72) and (105)
10. Use the control signal as the input of system (1)
11. Measure the system states and repeat steps 4 to 11

IV. SIMULATION RESULTS

To further demonstrate the effectiveness of the proposed algorithm, a mass-spring-damper [24] with friction shown in Fig. 3, is considered. The system dynamics can be expressed as:

$$\begin{aligned}&\dot{x}_1=x_2\\&\dot{x}_2=-\frac{1}{m}s(x_1)-\frac{1}{m}b(x_2)-\frac{1}{m}fr(x_2)+\frac{1}{m}v^{\sigma}\\&y=x_1\end{aligned}\tag{140}$$

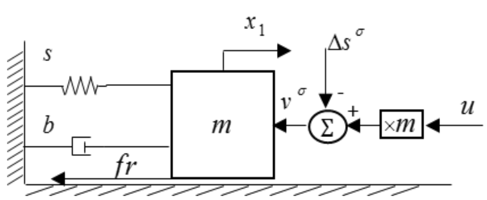

Fig. 3. Mass-spring-damper system.

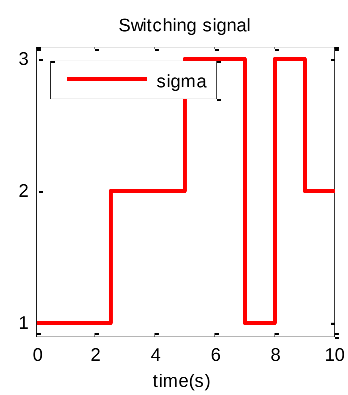

Fig. 4. Switching signal.

where x_1 and x_2 are the position and velocity of the mass *m*, respectively, s and b represent uncertain functions for spring and damper, respectively, fr denotes the friction, y is the output, and $v^{\sigma}=-\Delta s^{\sigma}(\bar{x}_2)+mu$ $(\sigma\in\{1,2,3\})$ are three predefined controllers that can be applied to the system, in which $\bar{x}_2 = [x_1 \ x_2]^T$, v is the new input, and Δs^{σ} is the switching signal shown in Fig. 4. By replacing u^{σ}, system (140) can be rewritten as

$$\begin{aligned} \dot{x}_1 &= x_2 \\ \dot{x}_2 &= -\frac{1}{m}[s(x_1) - fr(x_2) - \Delta s^{\sigma}(\bar{x}_2)] - \frac{1}{m}b(x_2) + v \\ y &= x_1 \end{aligned} \tag{141}$$

where $\Delta s^1 = x_1^3 \sin(x_1 x_2)$, $\Delta s^2 = x_2 \cos(x_1^2)$, $\Delta s^3 = x_2 x_1^2$, and $\Delta s^{\sigma}(0) = 0$ $(\sigma \in \{1, 2, 3\})$. Other parameters and functions are considered as follows:

$$m = 1/3 \text{ Kg}, \ s(x_1) = 2x_1^2, \ b(x_2) = x_2^2 \cos(x_2)$$

$$r_{11} = 3, \ r_{12} = 3.5, \ r_{21} = 12, \ r_{22} = 20, \ \eta_1 = \eta_2 = 1 \ \delta_{f1} = \delta_{f2} = 0.9, \ \lambda_{a1} = 15, \ \lambda_{a2} = 17, \ \lambda_{c1} = 12, \ \lambda_{c2} = 13$$

$$fr = 0.5mg(0.3 + 0.5e^{-(x2/0.9)^2} \tanh(5x2) + 0.8x2 \ \ \delta_{z1} = \delta_{z2} = \delta_{J1} = \delta_{J2} = 0.01.$$

The desired output is $y_d = 0.5\sin(4t)$. The initial weights for NNs are $W_{a1}(0) = [0.4 \cdots 0.4]^T \in R^{24\times1}$, $W_{c1}(0) = [0.1 \cdots 0.1]^T \in R^{24\times1}$, $W_{a2}(0) = [0.5 \cdots 0.5]^T \in R^{32\times1}$, $W_{c2}(0) = [0.3 \cdots 0.3]^T \in R^{32\times1}$, $\theta_1(0) = 0.05$, and $\theta_2(0) = 0.02$.

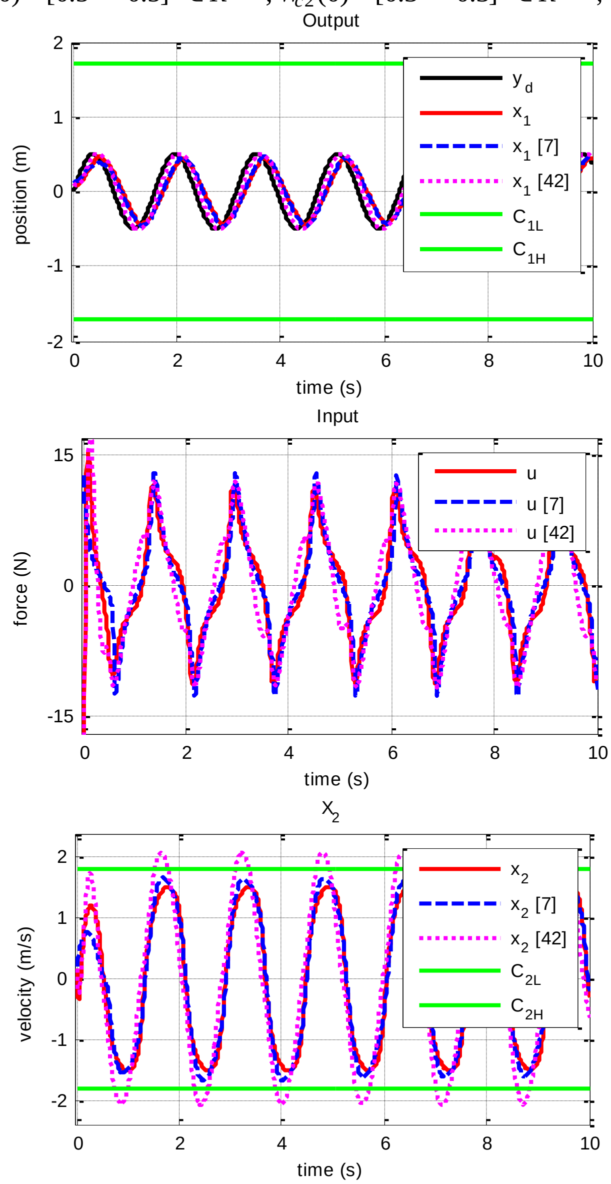

Fig. 5. Trajectories of states and input signal for symmetric time-invariant constraints.

To better highlight the advantages of the proposed controller, the results are compared with the methods introduced in [7] and [42]. In [7], a Tan-BLF approach is used to prevent violations of symmetric and time-invariant constraints in output-feedback systems. However, the input signal is not optimized. Moreover, it is assumed that all states are measurable. In [42], the optimized backstepping method is applied to control a state-feedback system with output hysteresis, but no state constraints are considered. For a fair comparison, the hysteresis effect is omitted.

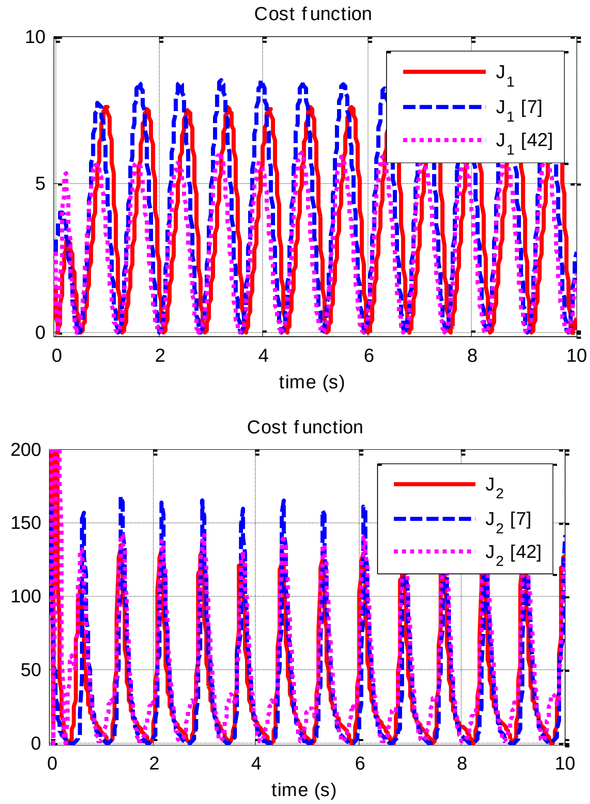

Fig. 6. Cost function for steps 1 and 2 of backstepping.

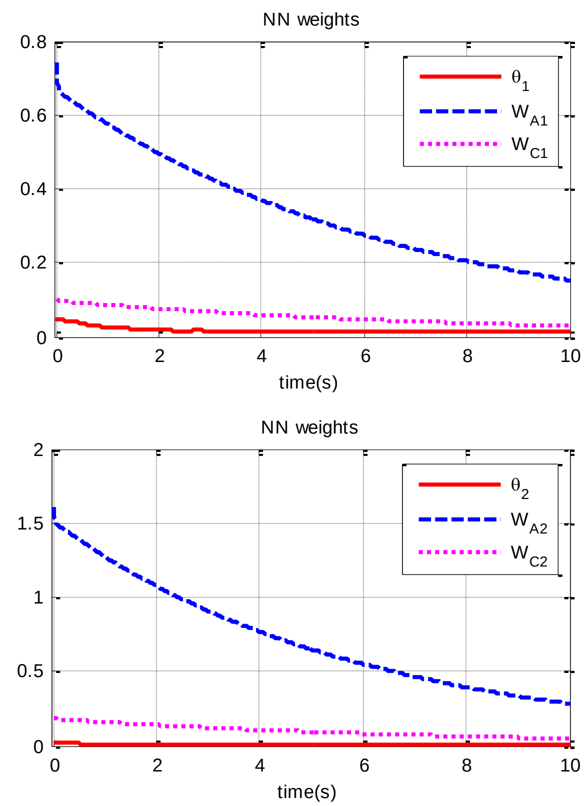

Fig. 7. Norm of the NN weights for step 1 and 2 of backstepping.

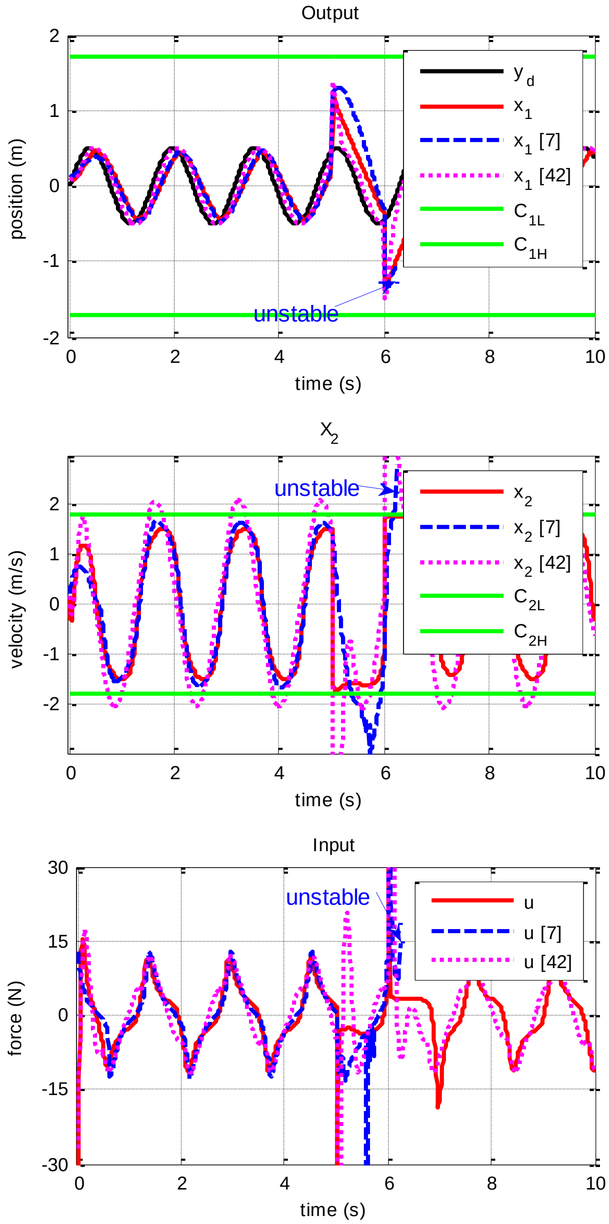

Fig. 8. Trajectories of states and input signals with disturbance.

To make the fair comparison, the constraints are first considered as $\underline{c}_1=\bar{c}_1=1.7$ and $\underline{c}_2=\bar{c}_2=1.8$, since the method in [7] can only handle symmetric and time-invariant constraints. The simulation results for the sinusoidal desired output are shown in Figs. 5–7. Fig. 5 shows the position and velocity of the mass with the imposed constraints and the controller input. As this figure shows, the controller in [42] violates the constraints, whereas the proposed controller and the method in [7] successfully maintain them. Fig. 6 shows the cost function for the two steps of the backstepping procedure for three methods. This figure reveals that the method in [7] has a higher cost function, due to its non-optimal method. Fig. 7 shows the norm of the NN weights.

To further evaluate the performance of the three methods, the disturbance-rejection and input-saturation results are shown in Figs. 8 and 9, respectively. In Fig. 8, a pulse disturbance with amplitude 1 is applied to the system output between 5 s and 6 s. As can be observed, the proposed method successfully maintains all constraints, while the method in [7] becomes unstable and the method in [42] violates the constraints. In Fig. 9, the input is saturated at 7 N. Similar to Fig. 8, the proposed method outperforms other two methods. To further demonstrate that the proposed method can perfectly handle time-varying as well as asymmetric constraints, it is also tested with $\underline{c}_1=-0.4\sin(4t)+0.5$, $\bar{c}_1=0.5\sin(4t)+0.3$, $\underline{c}_2=1.3$, and $\bar{c}_2=0.5\cos(4t)+0.7$. The results are shown in Fig. 10. As this figure shows, the method in [7] becomes unstable and the method in [42] violates the constraints.

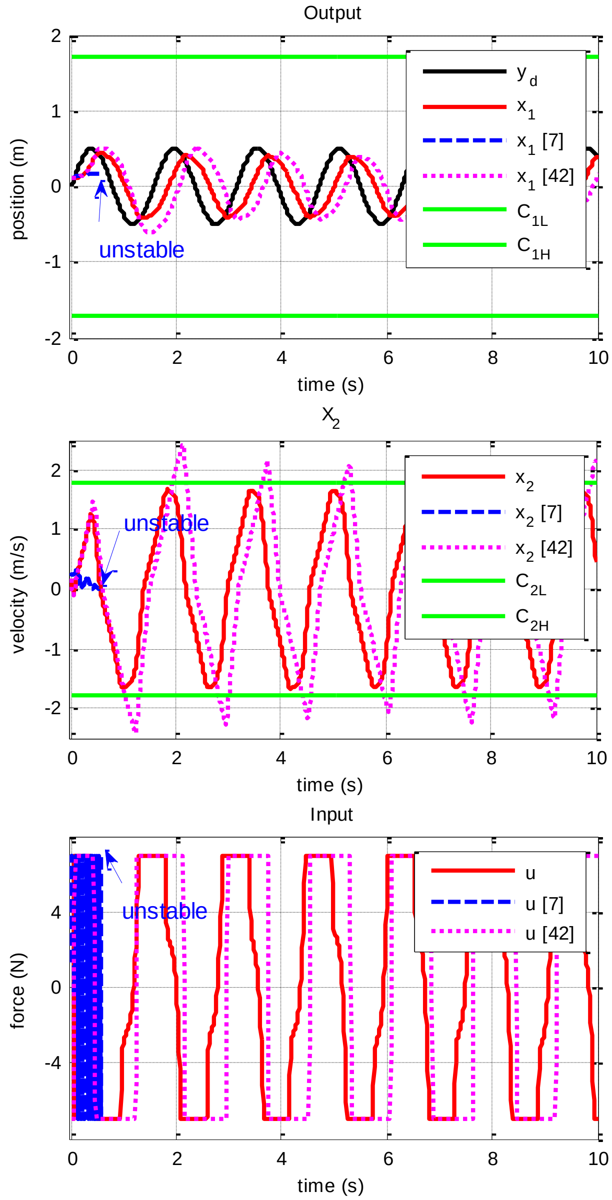

Fig. 9. Trajectories of states and input signals for saturated inputs.

V. CONCLUSION

In this study, an adaptive finite-time control scheme based on backstepping and NN techniques has been proposed for a class of strict-feedback switched systems subject to full-state asymmetric and time-varying constraints. By incorporating the NM approach into the backstepping framework, the boundedness of all closed-loop signals is ensured while satisfying the full-state constraints. This integration effectively relaxes the feasibility condition on the virtual controller, which is often difficult to achieve in conventional methods. The nonlinear functions are approximated using RBFNNs, and by designing the adaptive law based on the norm of the RBFNN weights, only one adaptive law per step is required, thereby reducing computational complexity. The optimization was performed using an actor–critic framework, in which the update laws for the actor–critic network weights are derived from the negative gradient of a positive-definite function obtained through the partial derivative of the HJB equation, thereby simplifying the overall model. Simulation results confirm the effectiveness and finite-time convergence of the proposed method. However, it should be noted that control schemes relying on BLF or NM may exhibit instability when the system constraints are temporarily violated. Future research should therefore focus on developing control strategies capable of maintaining system stability under temporary constraint violations. Moreover, the use of Young's inequality and squared Lyapunov functions introduces a certain degree of conservatism, which could be alleviated to enhance control performance. Finally, as the proposed optimized scheme is developed for a general mathematical model rather than a specific dynamic system, the design parameters are provided only within a range. For practical implementation, these parameters should be carefully tuned according to the characteristics of the actual system to ensure the best performance.

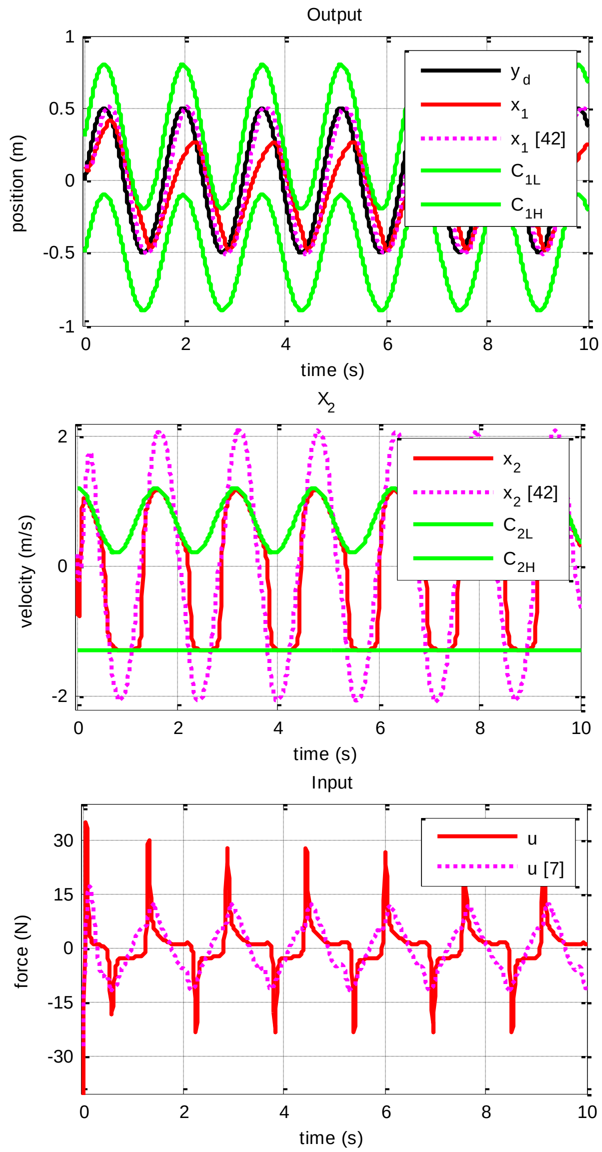

Fig. 10. Trajectories of states and input signals for asymmetric time-varying constraints.

REFERENCES

[1] Y. Liu, Z. Wang, L. Ma, Y. Cui, and F. E. Alsaadi, “Synchronization of directed switched complex networks with stochastic link perturbations and mixed time-delays,” *Nonlinear Anal.: Hybrid Syst.*, vol. 27, pp. 213–224, Feb. 2018.

[2] L. Long and T. Si, “Small-gain technique-based adaptive NN control for switched pure-feedback nonlinear systems,” *IEEE Trans. Cybern.*, vol. 49, no. 5, pp. 1873–1884, Apr. 2018.

[3] Y. Yin, B. Niu, X. Liu, X. Wang, and X. Jiang, “Adaptive intelligent-estimation-based tracking controller design strategy for switched nonlinear systems with unmodeled dynamics and an output constraint,” *ISA Trans.*, vol. 127, pp. 299–309, Aug. 2022.

[4] X. Zhao, Y. Kao, B. Niu, and T. Wu, *Control synthesis of switched systems*, Cham, Switzerland: Springer, 2017.

[5] S. Li, C. K. Ahn, and Z. Xiang, “Command-filter-based adaptive fuzzy finite-time control for switched nonlinear systems using state-dependent switching method,” *IEEE Trans. Fuzzy Syst.*, vol. 29, no. 4, pp. 833–845, Jan. 2020.

[6] W.-J. He, S.-L. Zhu, N. Li, and Y.-Q. Han, “Adaptive finite-time control for switched nonlinear systems subject to multiple objective constraints via multi-dimensional Taylor network approach,” *ISA Trans.*, vol. 136, pp. 323–333, May. 2022.

[7] H. Wang, W. Liu, and M. Tong, “Adaptive fuzzy fast finite-time output-feedback tracking control for switched nonlinear systems with full-state constraints,” *IEEE Trans. Fuzzy Syst.*, vol. 32, no. 3, pp. 958-968, Sep. 2023.

[8] M. Tong and H. Wang, “Observer-based adaptive fuzzy finite-time tracking control of switched nonlinear systems,” *Int. J. Syst. Sci.*, vol. 53, no. 11, pp. 2407–2420, Aug. 2022.

[9] K. He and L. Tang, “Adaptive event-triggered finite-time control for switched nonlinear systems,” *IEEE Trans. Fuzzy Syst*., vol. 32, no.3, pp. 745-754, Aug. 2023.

[10] K. P. Tee, S. S. Ge, and E. H. Tay, “Barrier Lyapunov functions for the control of output-constrained nonlinear systems,” *Automatica*, vol. 45, no. 4, pp. 918–927, Apr. 2009.

[11] Z.-L. Tang, K. P. Tee, and W. He, “Tangent barrier Lyapunov functions for the control of output-constrained nonlinear systems,” *IFAC Proc. Vol.*, vol. 46, no. 20, pp. 449–455, Jan. 2013.
[12] K. P. Tee and S. S. Ge, “Control of state-constrained nonlinear systems using integral barrier Lyapunov functionals,” in *Proc. 51st IEEE Conf. Decision Control (CDC)*, Maui, Hawaii, USA, 2012, pp. 3239-3244.
[13] T. Guo and X. Wu, “Backstepping control for output-constrained nonlinear systems based on nonlinear mapping,” *Neural Comput. Appl.*, vol. 25, pp. 1665–1674, Dec. 2014.
[14] Y. Liu and Q. Zhu, “Adaptive fuzzy asymptotic control for switched nonlinear systems with state constraints,” *Int. J. Syst. Sci*., vol. 53, no. 5, pp. 922–933, Apr. 2022.
[15] L. Tang, X.-Y. Zhang, Y.-J. Liu, and S. Tong, “Neural-network-based adaptive constrained control for switched systems under state-dependent switching law,” *IEEE Trans. Neural Netw. Learn. Syst*., vol. 34, no. 8, pp. 4057-4067, Oct. 2021.
[16] Y. Cao, N. Xu, H. Wang, X. Zhao, and A. M. Ahmad, “Neural networks-based adaptive tracking control for full-state constrained switched nonlinear systems with periodic disturbances and actuator saturation,” *Int. J. Syst. Sci*., vol. 54, no. 14, pp. 2689–2704, Oct. 2023.
[17] L. Liu, Z. Li, Y.-J. Liu, and S. Tong, “Adaptive fuzzy output feedback control of switched uncertain nonlinear systems with constraint conditions related to historical states,” *IEEE Trans. Fuzzy Syst*., vol. 30, no. 12, pp. 5091–5103, Apr. 2022.
[18] L. Tang, M. Yang, Y.-J. Liu, and S. Tong, “Adaptive output feedback fuzzy fault-tolerant control for nonlinear full-state-constrained switched systems,” *IEEE Trans. Cybern*., vol. 53, no. 4, pp. 2325-2334, Oct. 2021.
[19] L. Liu, A. Chen, and Y.-J. Liu, “Adaptive fuzzy output-feedback control for switched uncertain nonlinear systems with full-state constraints,” *IEEE Trans. Cybern*., vol. 52, no. 8, pp. 7340–7351, Jan. 2021.
[20] L. Liu, Y. Cui, Y.-J. Liu, and S. Tong, “Adaptive event-triggered output feedback control for nonlinear switched systems based on full state constraints,” *IEEE Trans. Circuits Syst. II, Exp. Briefs*, vol. 69, no. 9, pp. 3779–3783, May 2022.
[21] L. Tang, M. Yang, and J. Sun, “Adaptive fuzzy constraint control for switched nonlinear systems in nonstrict feedback form,” *Int. J. Adapt. Control Signal Process*., vol. 35, no. 8, pp. 1594–1611, Aug. 2021.
[22] L. Tang, K. He, Y. Chen, Y.-J. Liu, and S. Tong, “Integral BLF-based adaptive neural constrained regulation for switched systems with unknown bounds on control gain,” *IEEE Trans. Neural Netw. Learn. Syst*., vol. 34, no. 11, pp. 8579-8588, Mar. 2022.
[23] K. Zhao and Y. Song, “Removing the feasibility conditions imposed on tracking control designs for state-constrained strict-feedback systems,” *IEEE Trans. Autom. Control*, vol. 64, no. 3, pp. 1265–1272, Jun. 2018.
[24] X. Wang, W. Zhao, J. Xia, H. Shen, Z. Zhao, and L. Wang, “Event-triggered adaptive neural control for state-constrained switched nonlinear systems based on nonlinear shifting function technique,” *J. Franklin Inst*., vol. 360, no. 2, pp. 759–776, Jan. 2023.
[25] Z. Cao, B. Niu, G. Zong, and N. Xu, “Small-gain technique-based adaptive output constrained control design of switched networked nonlinear systems via event-triggered communications,” *Nonlinear Anal.: Hybrid Syst*., vol. 47, p. 101299, Feb. 2023.
[26] A. Moradvandi, S. A. Malek, and M. Shahrokhi, “Adaptive finite-time fault-tolerant controller for a class of uncertain MIMO nonlinear switched systems subject to output constraints and unknown input nonlinearities,” *Nonlinear Anal.: Hybrid Syst*., vol. 35, p. 100821, Feb. 2020.
[27] F. Cheng, H. Wang, G. Zong, B. Niu, and X. Zhao, “Adaptive finite-time command-filtered control for switched nonlinear systems with input quantization and output constraints,” *Circuits Syst. Signal Process*., vol. 42, no. 1, pp. 147–172, Jan. 2023.
[28] J.-J. Sun, S.-L. Zhu, Y.-Y. Guo, and Y.-Q. Han, “Adaptive finite-time tracking control utilising command filtering for a class of switched nonlinear systems subject to state constraints: facilitated by multi-dimensional Taylor network approach,” *Int. J. Control*, vol. 99, no. 1, pp. 37–48, Jan. 2026.
[29] S. Liu, H. Zhang, and H. Pang, “Finite-time adaptive fuzzy constrained control of uncertain switched nonlinear systems with zero dynamics,” *J. Franklin Inst*., vol. 362, no. 3, p. 107513, Feb. 2025.
[30] J.-J. Sun, S.-L. Zhu, Y.-Y. Guo, and Y.-Q. Han, “MTN-based adaptive finite-time tracking control for switched non-linear systems with time-varying state function constraints,” *Int. J. Adapt. Control Signal Process*., vol. 39, no. 4, pp. 724-735, Apr. 2025.
[31] F. L. Lewis, D. Vrabie, and V. L. Syrmos, *Optimal Control*. Hoboken, NJ, USA: Wiley & Sons, 2012.
[32] G. Wen, S. S. Ge, and F. Tu, “Optimized backstepping for tracking control of strict-feedback systems,” *IEEE Trans. Neural Netw. Learn. Syst*., vol. 29, no. 8, pp. 3850–3862, Mar. 2018.
[33] G. Wen, C. L. P. Chen, and S. S. Ge, “Simplified optimized backstepping control for a class of nonlinear strict-feedback systems with unknown dynamic functions,” *IEEE Trans. Cybern*., vol. 51, no. 9, pp. 4567–4580, Jul 2020.
[34] J. Zhang, K. Li, and Y. Li, “Output-feedback-based simplified optimized backstepping control for strict-feedback systems with input and state constraints,” *IEEE/CAA J. Autom. Sinica*, vol. 8, no. 6, pp. 1119–1132, May 2021.
[35] G. Wen, W. Hao, W. Feng, and K. Gao, “Optimized backstepping tracking control using reinforcement learning for quadrotor unmanned aerial vehicle system*,” IEEE Trans. Syst., Man, Cybern.: Syst*., vol. 52, no. 8, pp. 5004–5015, Sep. 2021.
[36] G. Wen and C. L. P. Chen, “Optimized backstepping consensus control using reinforcement learning for a class of nonlinear strict-feedback-dynamic multi-agent systems,” *IEEE Trans. Neural Netw. Learn. Syst*., vol. 34, no. 3, pp. 1524–1536, Aug. 2021.
[37] B. Dong et al., “Robust performance-prescribed attitude control of foldable wave-energy powered AUV using optimized backstepping technique,” *IEEE Trans. Intell. Veh*., vol. 8, no. 2, pp. 1230–1240, Jul. 2022.
[38] F. Shen, X. Wang, H. Li, and X. Yin, “Adaptive output-feedback control for a class of nonlinear systems based on optimized backstepping technique,” *Int. J. Adapt. Control Signal Process*., vol. 36, no. 5, pp. 1077–1097, May 2022.
[39] R. Zhou, G. Wen, and B. Li, “Reinforcement learning-based optimized backstepping control of nonlinear strict feedback system with unknown control gain function,” *Optim. Control Appl. Methods*, vol. 43, no. 5, pp. 1358–1378, Sep. 2022.
[40] G. Wen, B. Li, and B. Niu, “Optimized backstepping control using reinforcement learning of observer-critic-actor architecture based on fuzzy system for a class of nonlinear strict-feedback systems,” *IEEE Trans. Fuzzy Syst*., vol. 30, no. 10, pp. 4322–4335, Feb. 2022.
[41] Y. Qin, L. Cao, Q. Lu, and Y. Pan, “Reinforcement learning-based optimized backstepping control for strict-feedback nonlinear systems subject to external disturbances,” *Optim. Control Appl. Methods*, vol. 44, no. 5, pp. 2724-2743, Sep. 2023.
[42] L. Zheng, Z. Liu, C. L. P. Chen, Y. Zhang, Z. Wu, and S. Xie, “Adaptive fuzzy optimal control for switched nonlinear systems with output hysteresis,” *IEEE Trans. Fuzzy Syst*., vol. 31, no. 6, pp. 1940–1952, Oct. 2023.
[43] J. Ruan, Y. Fu, and Y. Fan, “Event-triggered adaptive neural network-based optimal control of strictly feedback switched nonlinear systems with state constraints,” *Int. J. Robust Nonlinear Control*, vol. 34, no. 18, pp. 11953–11984, Dec. 2024.
[44] B. Niu, Y. Liu, G. Zong, Z. Han, and J. Fu, “Command filter-based adaptive neural tracking controller design for uncertain switched nonlinear output-constrained systems,” *IEEE Trans. Cybern*., vol. 47, no. 10, pp. 3160–3171, Jan. 2017.
[45] Y. Liu, Q. Zhu, X. Zhou, and L. Wang, “Adaptive fuzzy tracking of switched nonstrict-feedback nonlinear systems with state constraints based on event-triggered mechanism,” *ISA Trans.*, vol. 121, pp. 30–39, Feb. 2022.
[46] C. Qian and W. Lin, “Non-Lipschitz continuous stabilizers for nonlinear systems with uncontrollable unstable linearization,” *Syst. Control Lett*., vol. 42, no. 3, pp. 185–200, Mar. 2001.
[47] Z.-Y. Sun, M.-M. Yun, and T. Li, “A new approach to fast global finite-time stabilization of high-order nonlinear system,” *Automatica*, vol. 81, pp. 455–463, Jul. 2017.